CR 151613

(NASA-CR-151613) Ku-BAND ANTENNA ACQUISITION AND TRACKING PERFORMANCE STUDY, VOLUME 4 (LinCom Corp., Pasadena, Calif.)
95 p HC A05/MF A01 CSCL 20N

N78-17252

Unclas
G3/32 05337

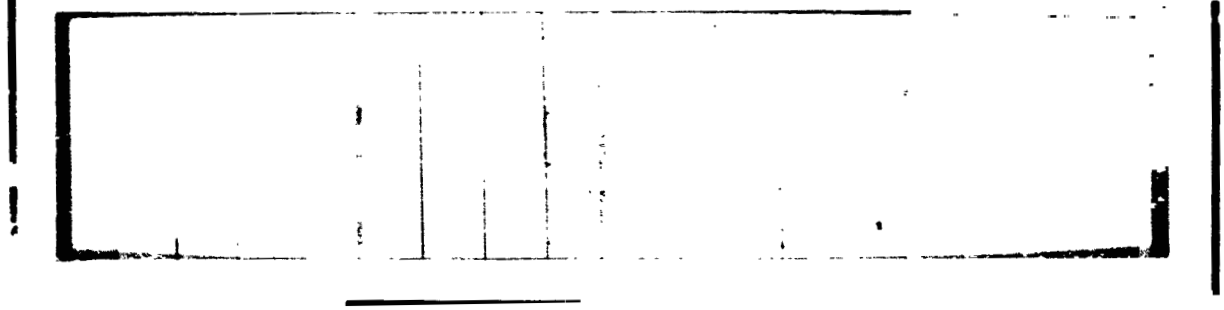

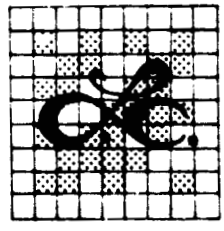

LinCom Corporation
PO Box 2793D, Pasadena, Calif 91105

LinCom

KU-BAND ANTENNA ACQUISITION AND TRACKING PERFORMANCE STUDY

VOLUME IV

Prepared for

NASA JOHNSON SPACE CENTER
HOUSTON, TX 77058

Technical Monitor: Jack Seyl

Contract Number NAS 9-14636

Prepared by

T. C. Huang
W. C. Lindsey

LINCOM CORPORATION
P.O. BOX 2793D
PASADENA, CA 91105

ORIGINAL PAGE IS
OF POOR QUALITY

OCTOBER 1977

TR No. 7810-0675

LinCom

KU-BAND ANTENNA ACQUISITION AND TRACKING PERFORMANCE STUDY

VOLUME IV

VOLUME IV: Ku-Band Antenna Acquisition and Tracking Performance Study

VOLUME V: Hardware Simulation of Shuttle Ku-Band Anten Acquisition

This two volume report documents the work accomplished during amended Phase II of Contract Number NAS 9-14636. The system tradeoff analysis and system performance study that led to three antenna pointing and acquisition algorithms for hardware simulation is provided in Volume IV. The construction of results obtained from the hardware simulation are described in Volume V. A high level software description and a detailed software documentation of the computer programs is to be found in Volume V. The first three volumes of this report documents the work accomplished during Phase I of this contract.

LINCOM CORPORATION
P.O. BOX 2793D
PASADENA, CA 91105

October 1977

ACKNOWLEDGEMENT

The authors wish to thank Mr. Jack Seyl of the Johnson Space Center for providing us with certain technical data pertaining to the Shuttle Ku-Band pointing system and for participating in various stimulating discussions thoughout the contract period.

TABLE OF CONTENTS

TABLE OF CONTENTS (Cont'd)

OBJECTIVES

LINCOMs overall objective under this contract was to develop a hardware simulation which could emulate the Shuttle's Ku-Band Antenna Pointing and Signal Acquisition System. The desire was to develop a simulation in which the antenna pattern, the TDRS search volume, the a priori probability distribution of TDRS satellite position relative to the Shuttle, and the antenna scan procedure could be selected for the purpose of predicting performance for various Shuttle/TDRS antenna pointing and acquisition scenarios.

The simulation was developed under the constaints of assuming a fixed network operation, the system must be real world implementable, it must be cost effective, the program execution time must not be excessive, the modulation technique is PN/BI-ϕ/BPSK, and optimum performance is desirable.

SUMMARY

This document presents the results pertaining to the trade-off analysis and performance of the Ku-Band Shuttle antenna pointing and signal acquisition system. The study was performed assuming the existance of various antenna scanning trajectories and various signal acquisition algorithms. The square, hexagonal and spiral trajectories were investigated assuming the TDRS postulated uncertainty region and a flexible statistical model for the location of the TDRS within the uncertainty volume. The scanning trajectories, Shuttle/TDRS signal parameters and dynamics and three signal acquisition algorithms were integrated into a hardware simulation discussed herein and documented in detail in Volume V. The hardware simulation is quite flexible in that it allows one to evaluate signal acquisition performance for an arbitrary (programmable) antenna pattern, a large range of C/N_0's, various TDRS/Shuttle a priori uncertainty distributions and three distinct signal search algorithms.

Based upon the data made available during this contract period, certain Ku-Band forward link signal threshold characteristics were studied. The antenna pointing and acquisition threshold is found to be less than 60 dB-Hz with an acquisition time dependent on the antenna scan procedure and acquisition algorithm implemented. Various techniques are discussed in this report and a computer program is presented from which these can be evaluated. It appears that there will be no problem in meeting the system

spec even in light of the uncertainty associated with the possibilities of antenna sidelobe acquisition. The details are provided herein. Assuming a single channel monopulse system and a 30 MHz IF bandwidth, a monopulse tracking loop bandwidth of one Hz, the monopulse tracking jitter is 0.11 degrees at C/N_0 = 54 dB-Hz. The Costas loop arm filter bandwidths can be chosen to be ten times the data rate such that no false-lock problem occurs during carrier acquisition. Assuming a loop bandwidth of B_L = 3 kHz, the loop jitter is 10 degrees at C/N_0 = 60.4 dB-Hz. Acquisition can be accomplished in less than 10 seconds.

For the purpose of antenna scanning analysis, a reference coordinate system, whose z-axis is in line with the center axis of a specified uncertainty cone of the TDRS position, is chosen for the relative relation between the TDRS and the Shuttle antenna. The scan path of the Shuttle antenna can be projected onto the (x,y) plane of the coordinate system; while the uncertainty cone of the TDRS position can be described by a circle in the (x,y) plane. The uncertainty in the position of the TDRS is modeled by a truncated Gaussian probability density p(x,y) with uncertainty parameters $\sigma_x^2 = \sigma_y^2 = \sigma^2$. By changing the value of this variance parameter, the model is sufficiently general to include a uniform distribution of TDRS position uncertainty ($\sigma_p=\infty$) to one which specifies the position with probability one ($\sigma_p=0$).

In the study of antenna scanning three types of trajectories are proposed and evaluated in terms of average scan time and the

structure of coverage over the uncertainty cone of the TDRS position. The analysis technique used for finding average scan time is discussed and an illustration of the technique for a specific type of scanning trajectories and motion of the Shuttle antenna is given. The results show that the spiral trajectories is in general better than the other two trajectories, especially for a constant velocity along a trajectory, since the path of a spiral trajectory (from the center of uncertainty cone to its edge) can be shorter than the other two.

From the Ku-band system specifications, it has been recognized that the variation of the received signal level at the Shuttle (due to TDRS EIRP path loss and antenna pointing loss variations) varies as much as 23 dB. If the antenna sidelobes are not sufficiently suppressed, a potential problem called sidelobe acquisition may cause the degradation in system performance. Therefore in this tradeoff analysis study, three different acquisition strategies are proposed and evaluated. The first acquisition strategy may be used for the case where the sidelobe acquisition does not impose a problem to the system. The other two strategies are primarily designed to avoid the sidelobe acquisition (especially the first sidelobe).

In this study, we assume that the first sidelobe of the Shuttle antenna is 17.5 dB suppression from the main lobe of the antenna so that we can study the effectiveness of the acquisition algorithm proposed. Surely, one should note that the sidelobe acquisition can be overcome by tapering down the sidelobes of the Shuttle antenna below 23 dB. However, it has been

ORIGINAL PAGE IS
OF POOR QUALITY

found that with one particular acquisition algorithm studied, a strong sidelobe of the antenna can speed spatial acquisition significantly.

The scan schemes and acquisition algorithms are all integrated by a computer simulation program. This software package, discussed in Vol. V, provides a useful tool for predicting the performance of the Ku-band antenna pointing system. Various options are available for users to do tradeoff studies on system parameters in designing an acquisition system. The software package has been tested on UNIVAC 1100 Series computers and verified with analytical results.

I. THE TDRS POSITION AND SHUTTLE ANTENNAS

1. Reference Coordinates

In establishing the Ku-band communication link between a Space Shuttle receiver and the TDRS, the Shuttle receiver must perform spatial search for the TDRS position. Initially, it is assumed that the transmitter antenna of the TDRS illuminates the Shuttle with a spread spectrum signal and also that the position of the TDRS is nearly stationary during the process of spatial search of the Shuttle antenna, since the TDRS dynamically is moving along a figure 8 trajectory slowly.

To discuss the spatial search of the Shuttle acquisition system, we shall establish a reference of coordinate systems. In this study it is assumed that the size and center of the uncertainty cone within which one can locate the TDRS, are known at each Shuttle receiver. The geometric diagram of Fig. 1 depicts in general the relative relation between the Shuttle receiver and the TDRS. However, for the convenience of references we adopt a coordinate system whose z-axis is in line with the direction of the center of the uncertainty zone. Denote Az to be azimuth coordinate and El to be elevation. We shall project Az and El onto a plane perpendicular to the z-axis, as shown in Fig. 2, so that the uncertainty zone can be confined to a circle whose radial coordinate represents Elevation and angle coordinate Azimuth. Throughout this report, we shall use this projected plane to discuss the spatial search of the Shuttle antenna.

ORIGINAL PAGE IS
OF POOR QUALITY

Figure 1. GEOMETRIC LOCATION OF THE TDRS WITH RESPECT TO A SHUTTLE

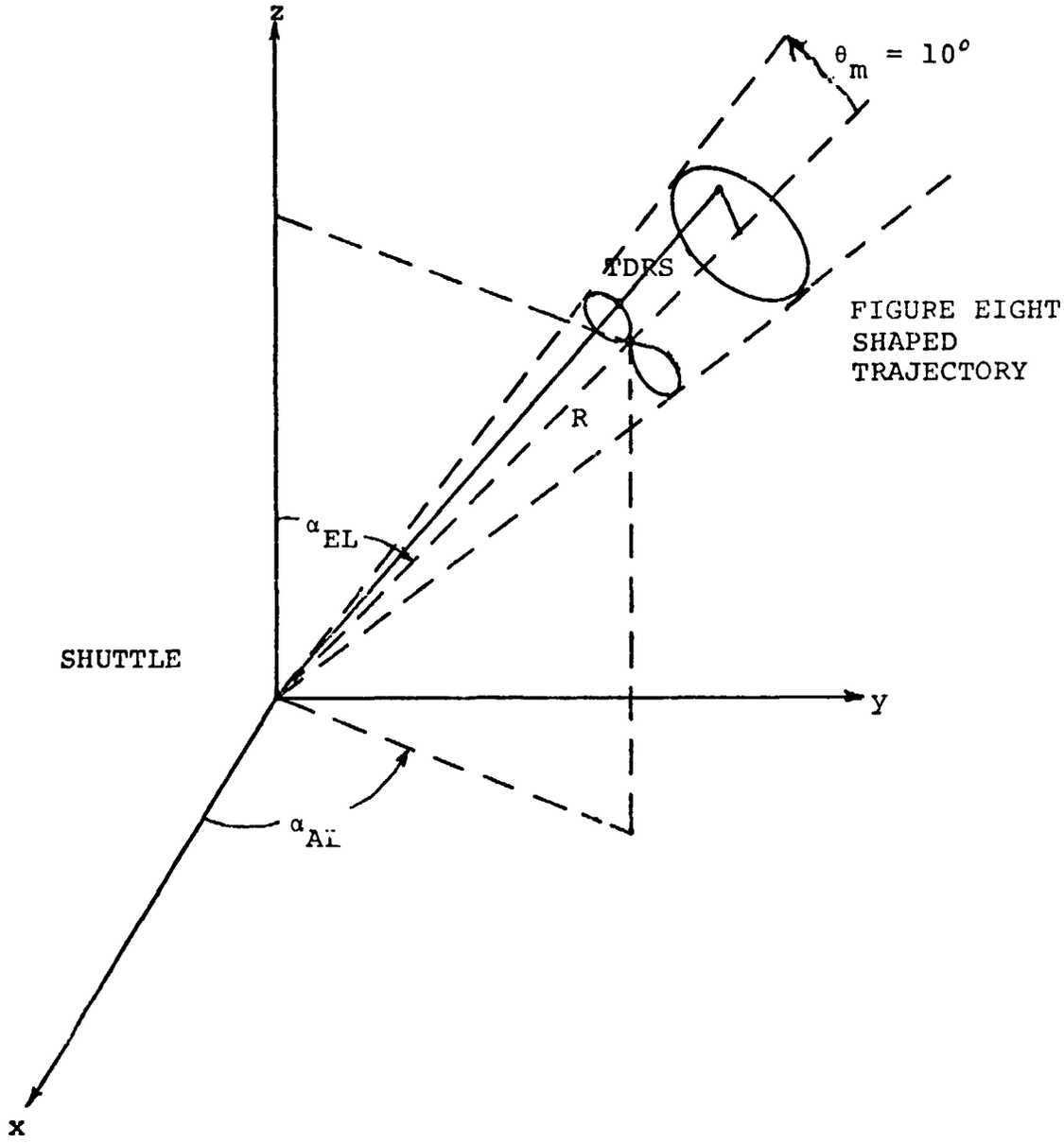

Figure 2. REFERENCE COORDINATE SYSTEM

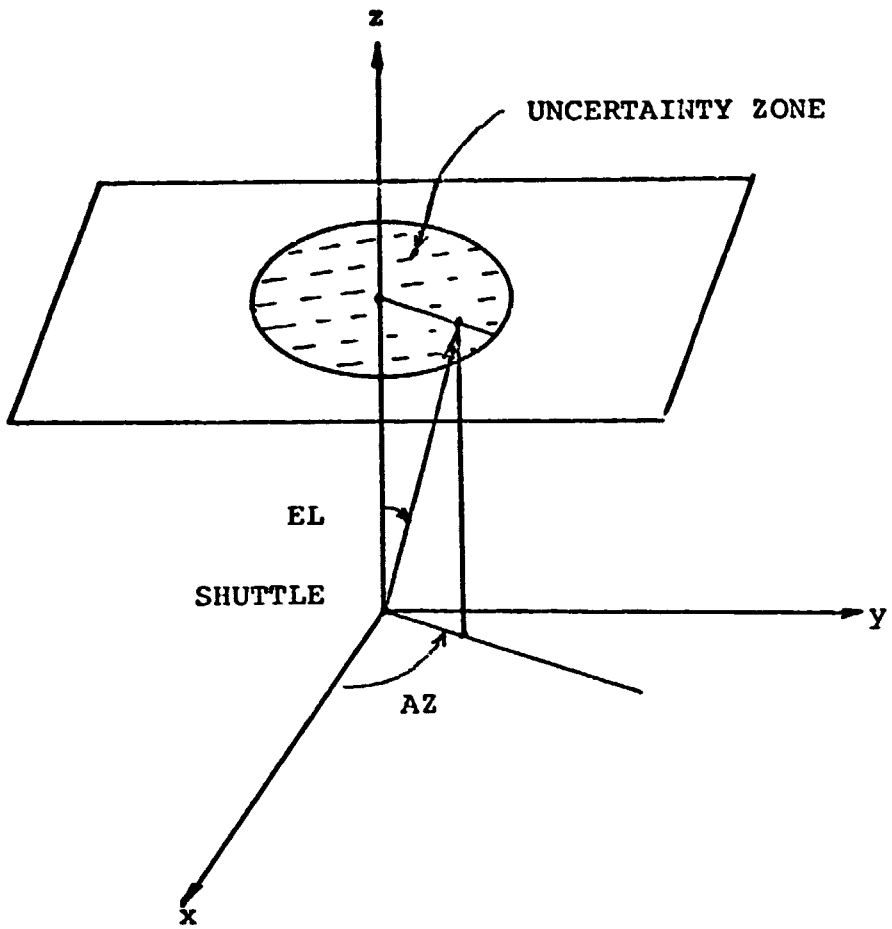

(a) Coordinate System in line with the center of the uncertainty zone TDRS.

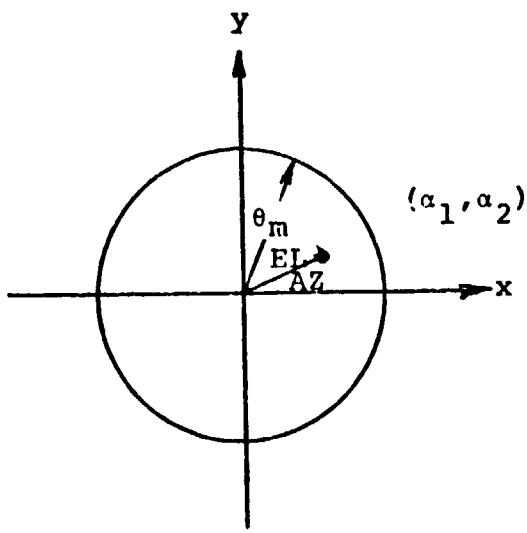

ORIGINAL PAGE IS
OF POOR QUALITY

(b) Projection of the TDRS uncertainty region onto a circle of radius θ_m

The position of the TDRS relative to the Shuttle receiver is only known up to a cone of angle θ_m. Nothing has been specified about the statistical distribution of the TDRS over the cone. In order to characterize its distribution, a "truncated" Gaussian function is assigned to (x-y) coordinates of the uncertainty zone on the projected plane. The "truncated" here means no tail for the Gaussian function, i.e., the probability of finding the TDRS at one point in x (or y) direction is of Gaussian form within the uncertainty region and zero outside the uncertainty zone. The value of variance σ_p of the Gaussian distribution reflects the statistical properties of finding the TDRS around the neighborhood of the center of uncertainty cone. The smaller the value of σ_p, the higher the chance of finding the TDRS near the center of the cone. For a higher value of σ_p, it approaches to a uniform distribution.

2. Statistical Model of the TDRS Position

Now the probability distribution is expressed in terms of (x-y) coordinates in the projected plane of Fig. 1b. The Gaussian distribution function is

$$\Phi(x,y) = \frac{1}{2\pi\sigma_p^2} \exp\left(-\frac{x^2+y^2}{2\sigma_p^2}\right) \qquad (1)$$

where σ_p^2 is the variance. The probability distribution of the TDRS at (x,y) is

$$f(x,y) = \begin{cases} k\Phi(x,y) & x^2+y^2 \leq \theta_m^2 \\ 0 & \text{elsewhere} \end{cases} \qquad (2)$$

where k is a normalized constant. One can show that

$$k = \frac{1}{1 - \exp\left(-\frac{\theta_m^2}{2\sigma_p^2}\right)} \tag{3}$$

by imposing the condition

ORIGINAL PAGE IS OF POOR QUALITY

$$\iint f(x,y)dxdy = 1 .$$

Note that the function $f(x,y)$ has the same zero mean as that of $\Phi(x,y)$, but it has different variance from σ_p^2. One can find that

$$\sigma_x^2 = \sigma_y^2 = \frac{k\sigma^2}{2}\left[1 - \left(1 + \frac{\theta_m^2}{2\sigma^2}\right)\exp\left(-\frac{\theta_m^2}{2\sigma^2}\right)\right] \tag{4}$$

In practice, it is more interesting to know the statistical characteristics along the direction of elevation and azimuth. One can express $f(x,y)$ in terms of polar coordinate system in the projected plane as follows

$$f(R,\theta) = \begin{cases} \frac{kR}{2\pi\sigma_p^2}\exp\left(-\frac{R^2}{2\sigma_p^2}\right) & 0 < R < \theta_m \\ 0 & \text{elsewhere} \end{cases} \tag{5}$$

where R is for elevation and θ for azimuth. It is obvious that the probability distribution in the azimuth is uniform over $(0,2\pi)$. Thus

$$f(R) = \begin{cases} \frac{kR}{\sigma_p^2}\exp\left(-\frac{R^2}{2\sigma_p^2}\right) & 0 < R < \theta_m \\ 0 & \text{elsewhere} \end{cases} \tag{6}$$

The mean and variance in the elevation can be shown to be

$$m_R = E(R)$$

$$= 2^{3/2} k\sigma_p \left[\frac{\sqrt{\pi}}{4} \operatorname{erf}\left(\frac{c_m}{\sqrt{2}\sigma_p}\right) - \frac{\theta_m}{2\sqrt{2}\sigma_p} \exp\left(-\frac{\theta_m^2}{2\sigma_p^2}\right)\right]$$

$$E(R^2) = k\sigma_p^2 \left\{ 1 - \left(1 + \frac{\theta_m}{2\sigma_p^2}\right) \exp\left(-\frac{\theta_m^2}{2\sigma_p^2}\right)\right\}$$

and

$$\text{Variance} = E(R^2) - m_R^2 \tag{7}$$

3. Mean, Variance and Moments for the TDRS Position

In order to show the relation between mean and variance of the elevation distribution and the variance σ_p^2, a tabulation of means and variances for different values of σ_p^2 is given in Fig. 3. In addition, because of the need in analyzing the average scan time, the moments of elevation and azimuth distributions are also tabulated in Fig. 4 (all normalized θ_m=1).

4. Shuttle Receiver Antenna Pattern Model

It is assumed here that the pattern of the Shuttle antenna has only one single pencil beam with the first sidelobe down 17.5 dB from the main lobe. The beam width shall be referred to as the 3 dB contour of the antenna pattern. The type of the antenna pattern assumed here can be characterized as follows:

$$G(\theta) = \frac{J_1(2a \cos \theta)}{a \sin \theta} \tag{8}$$

where

θ = angle offset of the boresight axis of the Shuttle antenna from the direction of the TDRS position

a = a parameter determined by 3 dB beamwidth of the antenna θ_s

Figure 3. MEAN AND VARIANCE OF ELEVATION ANGLE
($\theta_m = 10°$)

σ_p	1°	2°	3°	4°	5°	6°	7°	10°
Mean m_{α_1}	1.253°	2.506°	3.733°	4.719°	5.353°	5.739°	5.98°	6.33°
$\sigma^2_{\alpha_1}$	0.429°	1.717°	3.68°	5.136°	5.70°	5.851°	5.866°	5.773°
σ_{α_1}	0.655°	1.310°	1.918°	2.266°	2.388°	2.419°	2.422°	2.403°

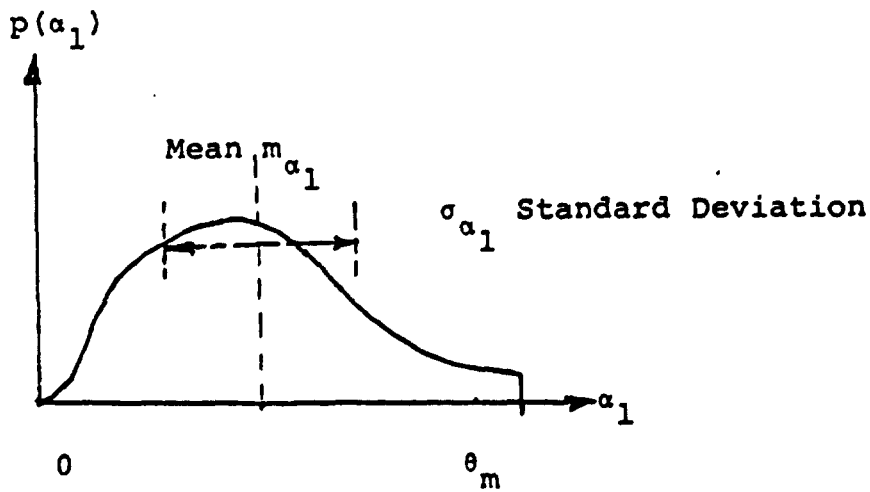

Figure 4. MEAN AND MOMENTS OF ELEVATION AND AZIMUTH DISTRIBUTION OF TDRS POSITION.

Elevation:

(I-1)TH CENTRAL MOMENTS

1	1.0000000E+00	
2	3.1307825E-01	Mean
3	2.6646434E-02	
4	2.6520391E-03	
5	2.2308420E-03	
6	6.2739134E-04	
7	3.5791496E-04	
8	1.5581140E-04	
9	8.4715485E-05	
10	4.4132538E-05	
11	2.4764277E-05	
12	1.40-0367E-05	
13	8.1651569E-06	
14	4.8283923E-06	
15	2.9042068E-06	

Azimuth:

MEAN, AND CENTRAL MOMENTS

MEAN=	5.0000000E-01
3	8.3333333E-02
4	0.
5	1.2500000E-02
6	0.
7	2.2321429E-03
8	0.
9	4.3402778E-04
10	0.
11	8.8778409E-05
12	0.
13	1.8780048E-05
14	0.
15	4.0690104E-06

ORIGINAL PAGE IS
OF POOR QUALITY

$J_1(x)$ = Bessel function of first-order

Note that here we assume the antenna pattern is spherically symmetric with respect to the boresight of the antenna. The function $2|J_1(x)|/x$ is plotted in Fig. 5. From the function one can see that the 3 dB point of the pattern is located at $x = 1.61$ and that the first sidelobe peak is 17.5 dB down from the main peak and occurs at $x = 5.1$. With this information one can design the antenna with 3 dB beamwidth by choosing the parameter a to satisfy the condition

$$a = \frac{1.61}{2 \sin \theta_B} \approx \frac{0.805}{\theta_B} \qquad (9)$$

where

θ_B = half beamwidth (in rad.)

In what follows we set a=57.65 and this gives rise to a beamwidth of 1.6°. The antenna pattern used in this study is plotted in Fig.6 with an amplifition factor of 3 in angle and in Fig. 7 in rectangular form. Note that the first null point of the main lobe is at $\theta_N = 1.78°$ and that the angle of the first sidelobe peak is $\theta_S = 2.5°$.

The function $G(\theta)$ gives the loss in the received signal power when the angle θ is nonzero. The θ, an offset angle, is an angle of the boresight axis of the Shuttle antenna off from the TDRS. To compute θ, one should know the relative geometric relation between the TDRS and Shuttle receivers. Using spherical coordinate system, we denote $\vec{A}$ to be a fector pointing toward the TDRS with unit magnitude, say $(1, \alpha_{AZ}, \alpha_{EL})$ and $\vec{B}$ be a unit vector in line with the boresight axis of the Shuttle antenna, say

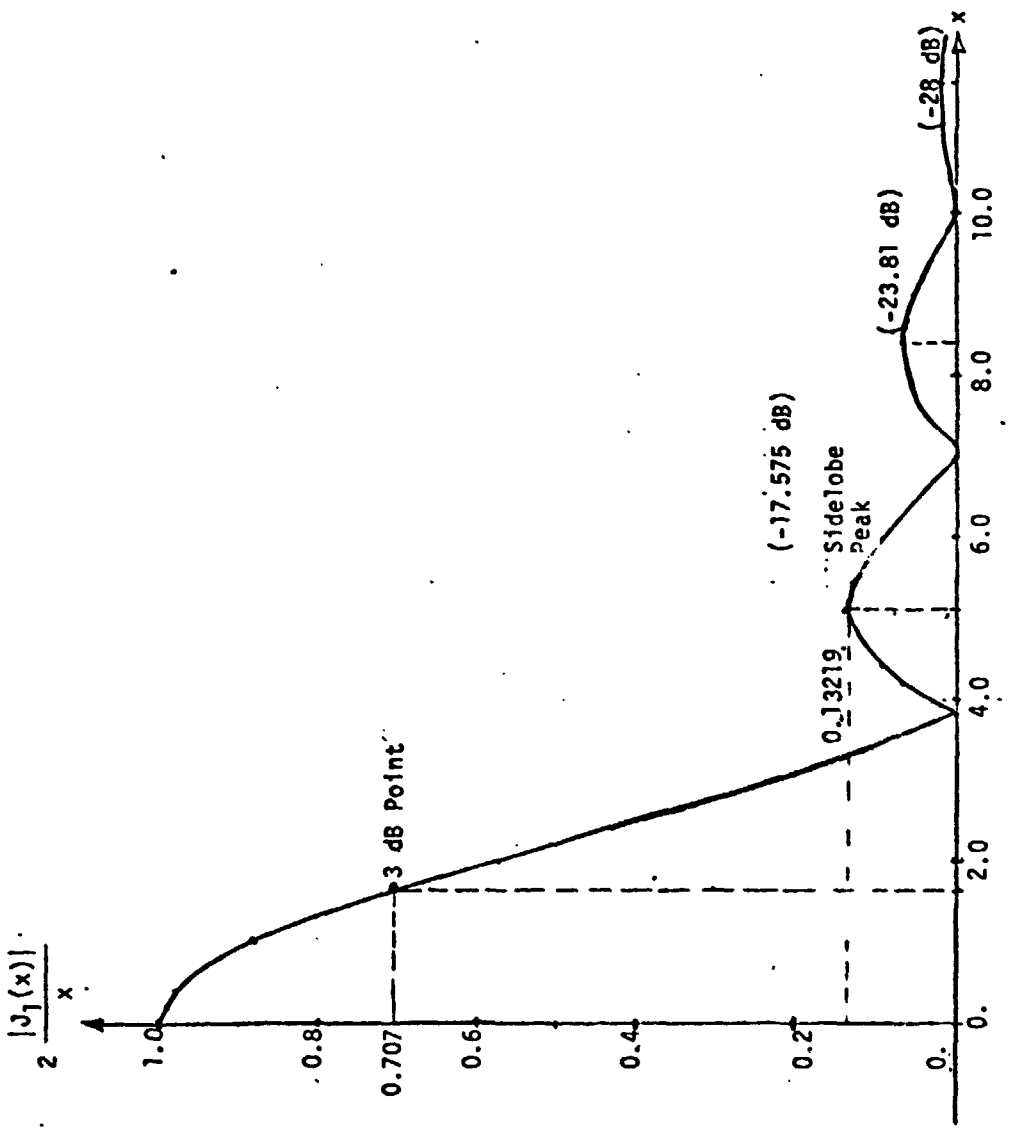

Figure 3. The Function - $\frac{2|J_1(x)|}{x}$

ORIGINAL PAGE IS
OF POOR QUALITY

Figure 5. Antenna Gain in Rectangular Coordinates.

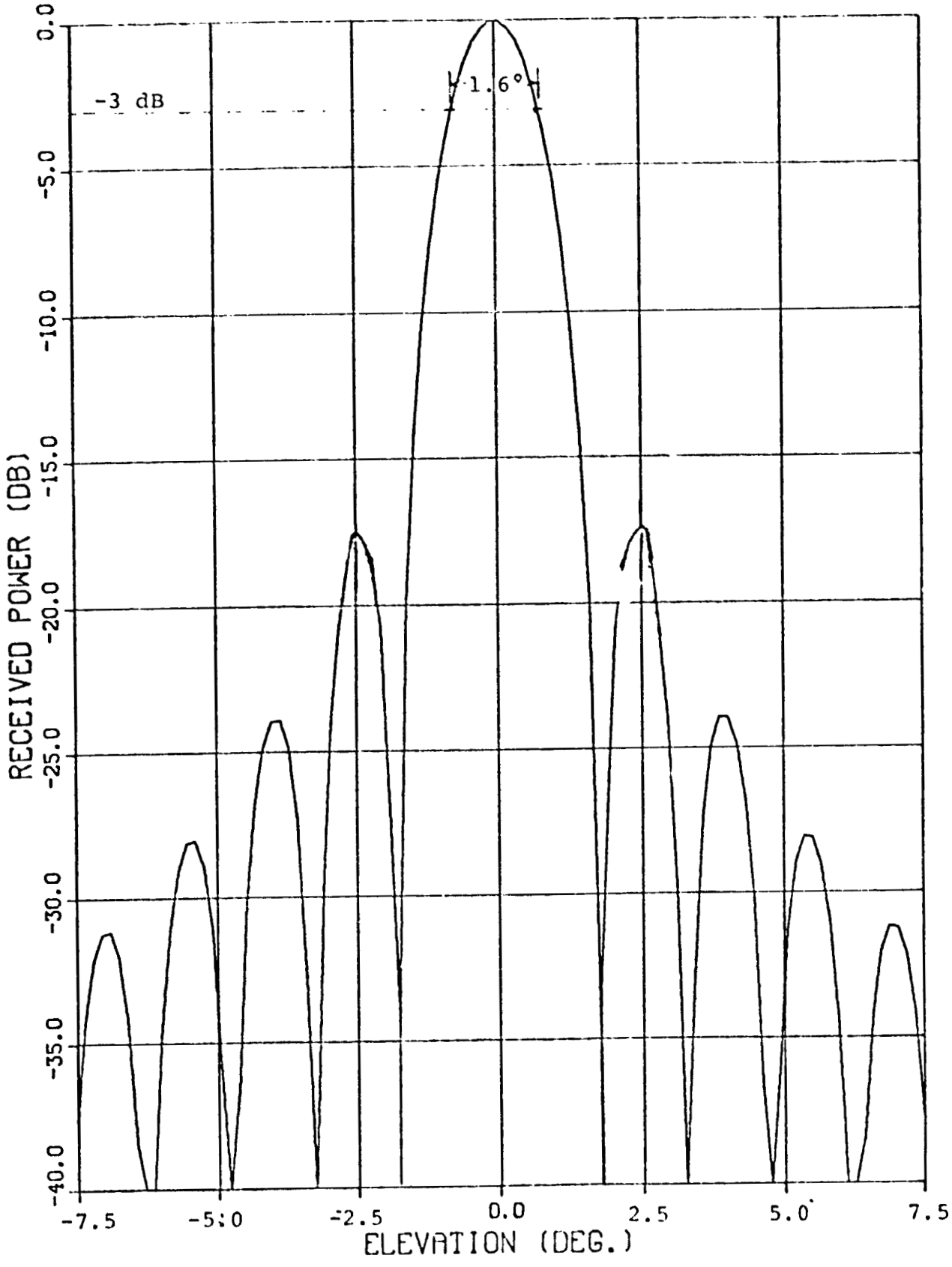

Figure 6. ANTENNA PATTERN

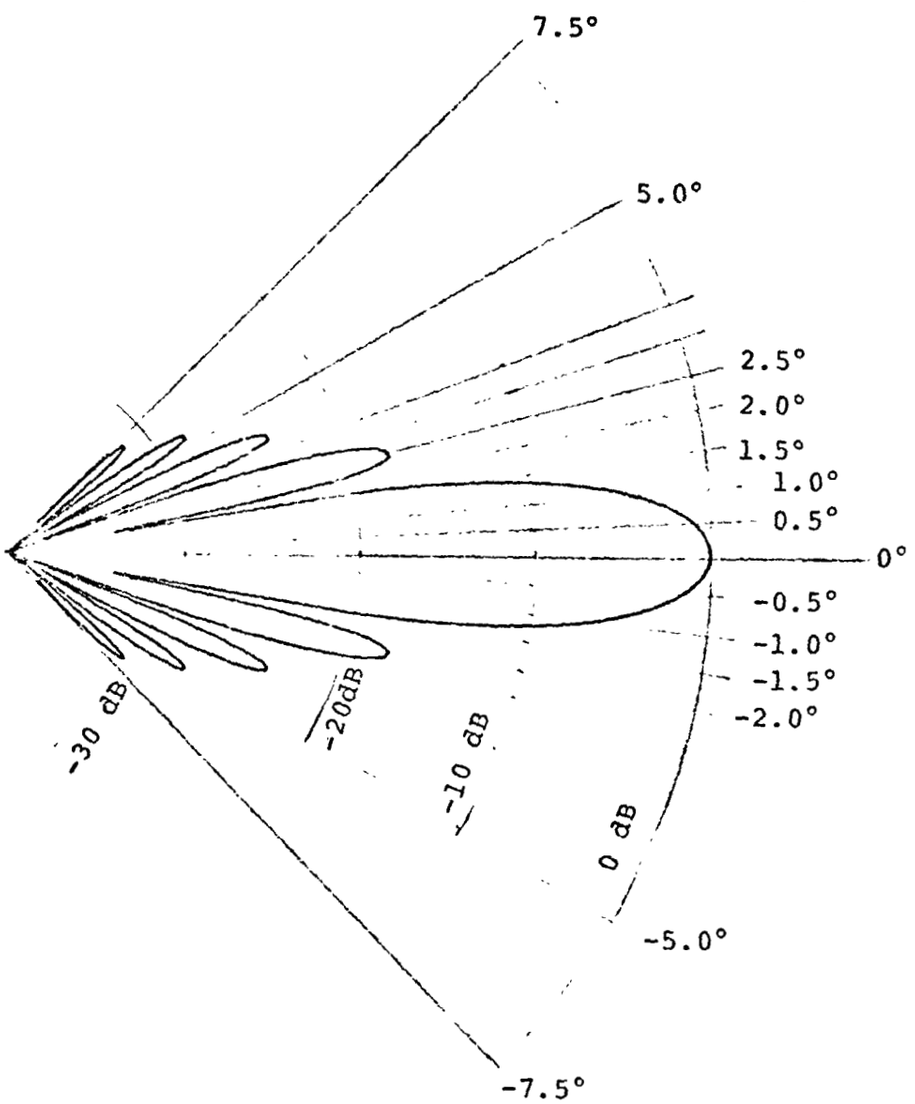

ANGLE = 6. ACTUAL SCALE

ORIGINAL PAGE IS
OF POOR QUALITY

$(1, \beta_{AZ}, \beta_{EL})$. Then one can express the offset angle θ to be

$$\cos\theta = \frac{\vec{A}\cdot\vec{B}}{|A||B|}$$

where

$|x|$ = length of a vector $\vec{X}$

$\cdot$ = scalar product of two vectors

In scalar form the above equation becomes

$$\cos\theta = \cos(\alpha_{AZ}-\beta_{AZ}) \sin\alpha_{EL} \sin\beta_{EL} + \cos\alpha_{EL} \cos\beta_{EL} \qquad (10)$$

If the TDRS happens to be at the center of uncertainty region, i.e., $\alpha_{AZ} = 0$ and $\alpha_{EL} = 0$, one immediately has

$$\cos\theta = \cos\beta_{EL} \text{ or } \theta = \beta_{EL}$$

Eq. (10) will be used in general to compute the offset angle θ for a given position of the TDRS and the direction of the boresight axis of Shuttle antennas. The latter will be represented as a point in the projected plane as indicated in Fig. 2b.

II. SPATIAL SCANNING OF SHUTTLE ANTENNA

1. Scanning Trajectories

In order to search spatially for the TDRS position systematically, one should assign a regular path for the Shuttle antenna to sweep across the uncertainty region. Projecting the path, along which the Shuttle antenna sweeps through, onto the plane perpendicular to the z-axis, we have a trajectory for the tip of boresight of the antenna and footprints for the 3 dB contour of the antenna pattern. To guarantee a complete coverage of the uncertainty region with a 3 dB contour footprint, one should properly design the trajectory. In this study, three kinds of scan trajectories are studied, viz.,

(1) Square Trajectory.

(2) Hexagonal Trajectory.

(3) Achimede Spiral Trajectory.

The characteristics of each trajectory will be discussed separately. Here we'll point out that the first two trajectories will have uniform overlaps between any two 3 dB contour of the antenna pattern. The whole uncertainty area is divided into cells inside which every point can be illuminated by at least a 3 dB contour of the Shuttle antenna. On the other hand, the third trajectory will have nonuniform overlaps, especially those cells near the center of the uncertainty zone. The overlap used here is defined to be the ratio of the portion of the overlap of two cells whose centers on a trajectory are aligned in the same radical direction, to the 3 dB beamwidth of the antenna, as shown in Fig. 8.

ORIGINAL PAGE IS
OF POOR QUALITY

Figure 8. DEFINITION OF OVERLAPS BETWEEN SEARCH CELLS

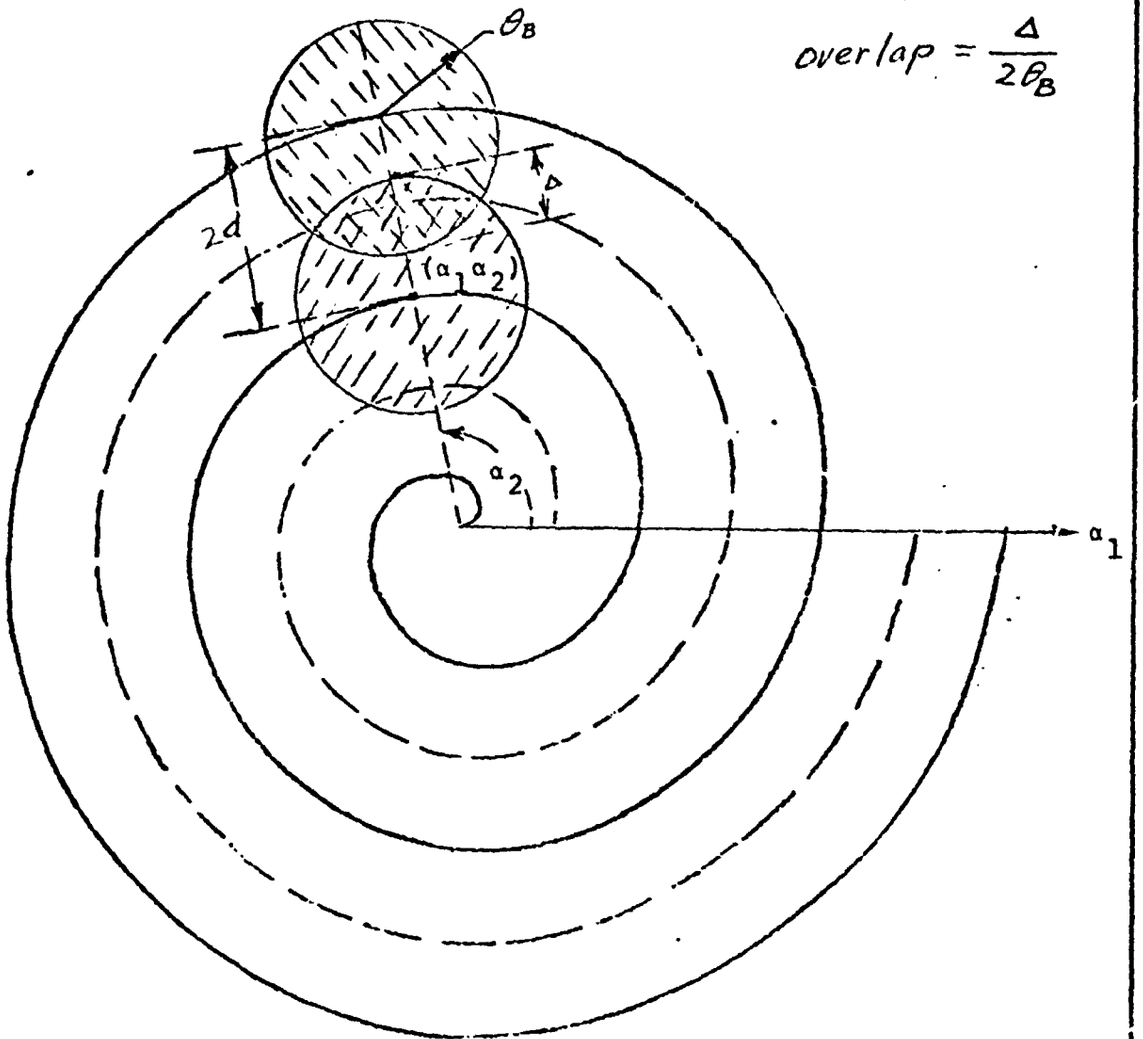

$$\alpha_1 = k_s \alpha_2$$

ORIGINAL PAGE IS
OF POOR QUALITY

$$\text{Overlap} = \frac{\Delta}{2\theta_B} \tag{11}$$

Here we also assume that all trajectories start at the center of the uncertainty cone.

(a) Square Trajectory

As the name implies, the trajectory is square-shaped and the uncertainty area is divided into square cells with diagonals $2\theta_B$, as shown in Fig. 9. The center of each cell can be easily determined from the geometry of the trajectory. One can see that the disadvantage of the square trajectory is that some of the cells are outside the specified uncertainty cone. Obviously one can easily determine the number of terms of the trajectory and the number of cells needed in order to completely cover the whole uncertainty cone.

Let θ_m be the angle of half the uncertainty cone, 2d the separation between two square cells, $2d = \sqrt{2}\theta_B$ and N the number of turns. Then from observation of geometry, one can easily express

$$\theta_B + 2Nd \geq \theta_m$$

or

$$N \geq \frac{\theta_m - \theta_B}{\sqrt{2}\theta_B} = \frac{1}{\sqrt{2}}\left(\frac{\theta_m}{\theta_B} - 1\right) \tag{12}$$

This indicates that it takes about $\frac{1}{\sqrt{2}}(\theta_m/\theta_B - 1)$ turns of square trajectory to sweep through the whole area. One may also estimate the number of cells needed

$$N_c = 1 + 8 + 2x8 + \ldots + 8xN$$
$$= 1 + 4N(N+1) \tag{13}$$

Figure 9. SQUARE SCANNING TRAJECTORY

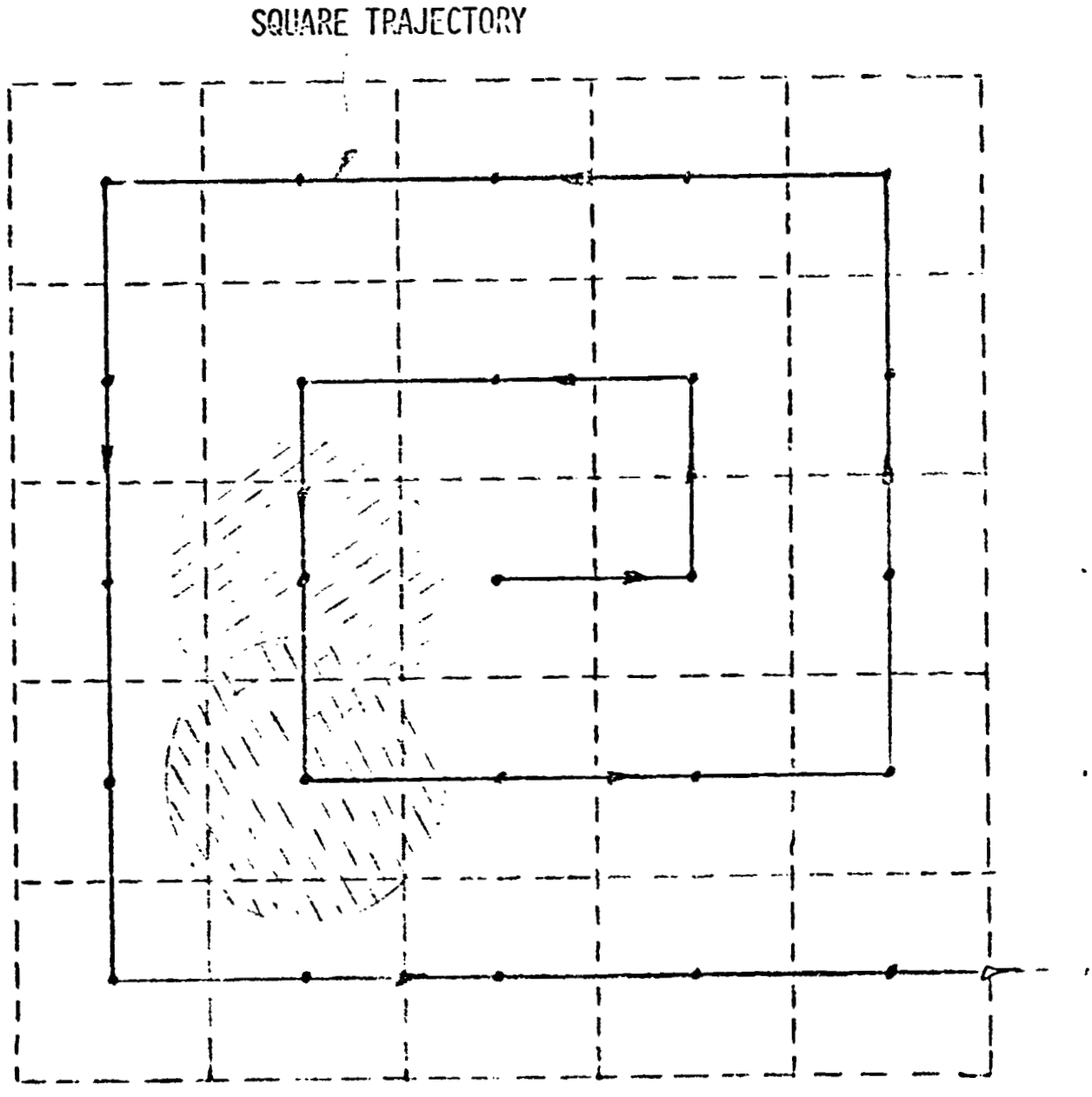

ORIGINAL PAGE IS
OF POOR QUALITY

For instance, $\theta_B = 0.8°$, $\theta_m = 10°$, then one needs

$$N \geq 8.13 \Longrightarrow \text{at least } N = 9 \text{ turns}$$

and the number of cells

$$N_c = 1 + 4 \times 9 \times 10 = 361 \text{ cells}$$

Finally, one should note that the overlap for the square trajectory is 29.3%.

(b) Hexagonal Trajectory

Hexagonal trajectory requires less overlap between cells. The intersections with all neighborhood cells are the six vertices of hexagons which form a honey comb. The separation 2d between two hexagonals is $\sqrt{3}\theta_B$, as shown in Fig. 10. Obviously, the centers of the cells can also be determined easily. Here we can also estimate the number of turns required to sweep the uncertainty area to be as

$$[\theta_B^2 + (2Nd)^2]^{1/2} \geq \theta_m$$

ORIGINAL PAGE IS
OF POOR QUALITY

one can solve for N

$$N \geq \frac{\sqrt{\theta_m^2 - \theta_B^2}}{2d} = \frac{1}{\sqrt{3}} \sqrt{\left(\frac{\theta_m}{\theta_B}\right)^2 - 1} \qquad (14)$$

The number of cells can also be computed

$$N_c = 1 + 6 + 2 \times 6 + \ldots + N \times 6$$

or

$$N_c = 1 + 3N(N+1) \qquad (15)$$

Comparing eq. (13) with (15), one can see that the number of

Figure 10. HEXAGONAL SCANNING TRAJECTORY

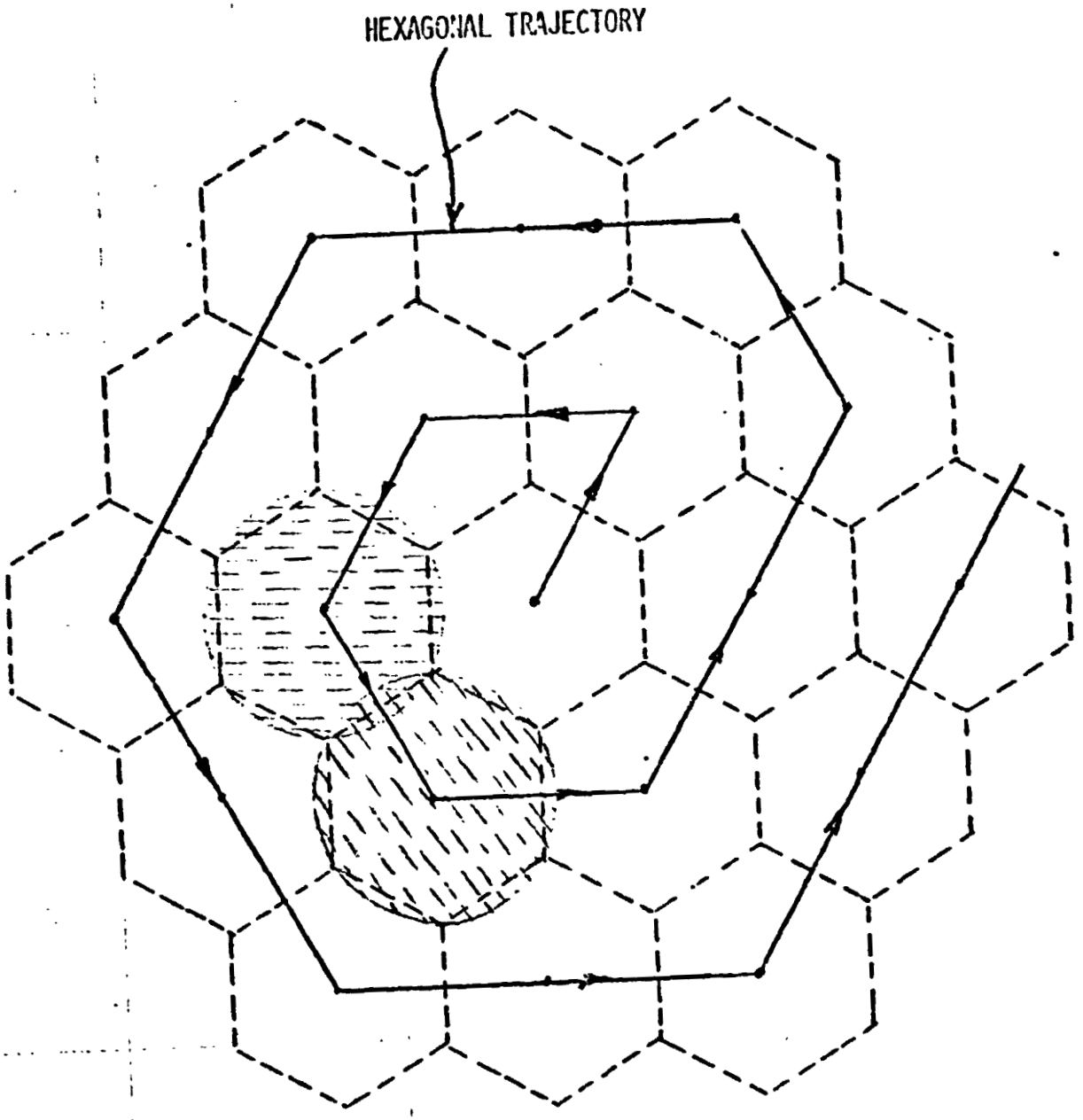

ORIGINAL PAGE IS
OF POOR QUALITY

cells required for the hexagonal trajectory is less than those for the square trajectory. say $\theta_B = 0.8°$ and $\theta_m = 10°$, the trajectory needs

$$N \geq 7.1 \Longrightarrow \text{at least } N = 8 \text{ turns}$$

and

$$N_c = 216 \text{ cells}$$

which is smaller than that for the square trajectory.

(c) Archimede Spiral Trajectory

When the boresight axis of the Shuttle antenna sweeps along a trajectory, the foot prints of a 3 dB contours of the antenna cover a uniform strip of area along the path. In order to utilize this fact, the Archimede spiral is most suitable because of its equal separation between trajectories. The Archimede spiral can be characterized as

$$El = \frac{d}{\pi} Az \ , \text{ or } \alpha_1 = k\alpha_2 \qquad (16)$$

where

$2d$ = separation between trajectory

Note that the variable α_2 (or Az) in the expression should not be limited to a range of 2π. According to the definition of overlap eq. (11), the separation d should be determined once the overlap of cells is specified.

Unlike other two trajectories, the spiral trajectory lacks geometrical symmetricity. So how to choose the center of cells to ensure a complete coverage of the scanned area becomes a nontrivial problem.

To explain the scheme of finding centers of cells along the

spiral, we shall start the first cell of the scan at El = 0 and Az = 0 and proceed along the spiral. We should impose a condition that the circle of the second cell passes through the intersection of the circle of the first cell and an auxiliary spiral. This auxiliary spiral falls in the Archimede spiral trajectory and can be characterized as below

$$\alpha_1 = \frac{d}{\pi} \alpha_2 + d \qquad (17)$$

as shown in Fig. 8.

Let A be the intersection point of the first cell and the auxiliary spiral, (El_{m1}, Az_{m1}), and B the center of the second cell (El_2, Az_2). Using eqs. (16) and (17), one can solve for El_{m1}, Az_{m1} and EL_2, Az_2 in sequence,

$$El_{m1} = \theta_B \text{ and } Az_{m1} = \frac{\pi}{d} (\theta_B - d) \qquad (18)$$

and

$$Az_{m1} = 2El_{m1} \cos(Az_2 - Az_{m1}) \qquad (19a)$$

$$El_2 = \frac{d}{\pi} Az_2 + d \qquad (19b)$$

The relation (19a) is derived from the fact that the distance from point A to B is θ_B. Combining two equations (19), one can iteratively solve for Az_2, then El_2. Repeating this procedure, one can find the centers of all cells to cover completely the scanned area. Here we shall formulate the general method.

Let the center of the $k^{\underline{th}}$ cell be known (El_k, Az_k). To find the center of the next cell $((k+1)^{\underline{th}})$ one should find the intersection of the circle of the $k^{\underline{th}}$ cell and the auxiliary spiral curve first. Denote the intersection to be (El_{mk}, Az_{mk}).

Then one can have the relation

$$Az_{mk} = Az_k + \cos^{-1}\left(1 - \frac{\theta_B^2-(El_{mk}-El_k)^2}{2El_{mk}El_k}\right) \quad (20)$$

to solve for Az_{mk}. Using eq. (17) one can compute El_{mk}. After obtaining the values of Az_{mk} and El_{mk}, one can solve for $Az_{(k+1)}$, iteratively, by the relation

$$Az_{(k+1)} = Az_{mk} + \cos^{-1}\left(1 - \frac{\theta_B^2-(El_{(k+1)}-El_{mk})^2}{2El_{(k+1)}El_{mk}}\right) \quad (21)$$

Similarly, one can obtain $El_{(k+1)}$ by eq. (17).

From the above discussion of finding centers of all cells one can realize that it is rather complicated to analytically evaluate the number of cells required or number of turns needed to cover whole area of uncertainty cone. However, a computer program implementing the above scheme has been developed and can provide those answers for a specified uncertainty cone.

(2) Motion of the Shuttle Receiver Antenna

Once a trajectory of spatial search is chosen for Shuttle receiver antennas, one needs to determine what type of motion should be used in order to meet aspects of the total search time. Here, it is assumed that the receiver antenna can be moved either in a constant angular velocity or constant speed in any trajectory or a combination of them. The constant angular velocity can be characterized as

$$\frac{d\alpha_2}{dt} = \text{constant} \quad (22)$$

ORIGINAL PAGE IS
OF POOR QUALITY

and the constant speed along a trajectory is defined to be

$$\left.\frac{ds}{dt}\right|_{\text{along trajectory}} = \text{constant} \qquad (23)$$

where s is the arc length along a trajectory.

How should we choose the type of motion for the receiver antenna depends on the flexibility of gimbol systems, which drive the antenna to sweep, on the adoption of scanning trajectories and on the consideration of dwell time for each search cell. One important parameter in the design of acquisition system is the total scan time. Here we shall discuss the effect of types of motion on the scan time. We shall neglect the time required for signal detection since it is normally much shorter than the time for mechanical motion.

Suppose that the beamwidth of the Shuttle antenna is 1.6°. the scan times to sweep over an uncertainty cone of 20° are plotted in Fig.11 for constant angular velocity of Shuttle antennas with the spiral trajectory. For instance, for a constant rotation speed of 100°/sec, it will take 32 seconds to sweep the whole uncertainty area if the overlap of the spiral trajectory is 30%. To meet the required scan time, 55 sec, it is necessary for the Shuttle antenna to rotate at least 50°/sec, for 15% of overlap spiral trajectory. This is equivalent to 0.131 cycle/sec. The scan times for other two types of trajectories are also shown in Fig. 11.

On the other hand, the curves given in Fig.12 show the scan time for constant speed along the trajectory. Note that the unit of speed is the same as the unit in elevation

Figure 11. Scan Time for Constant Angular Velocity.

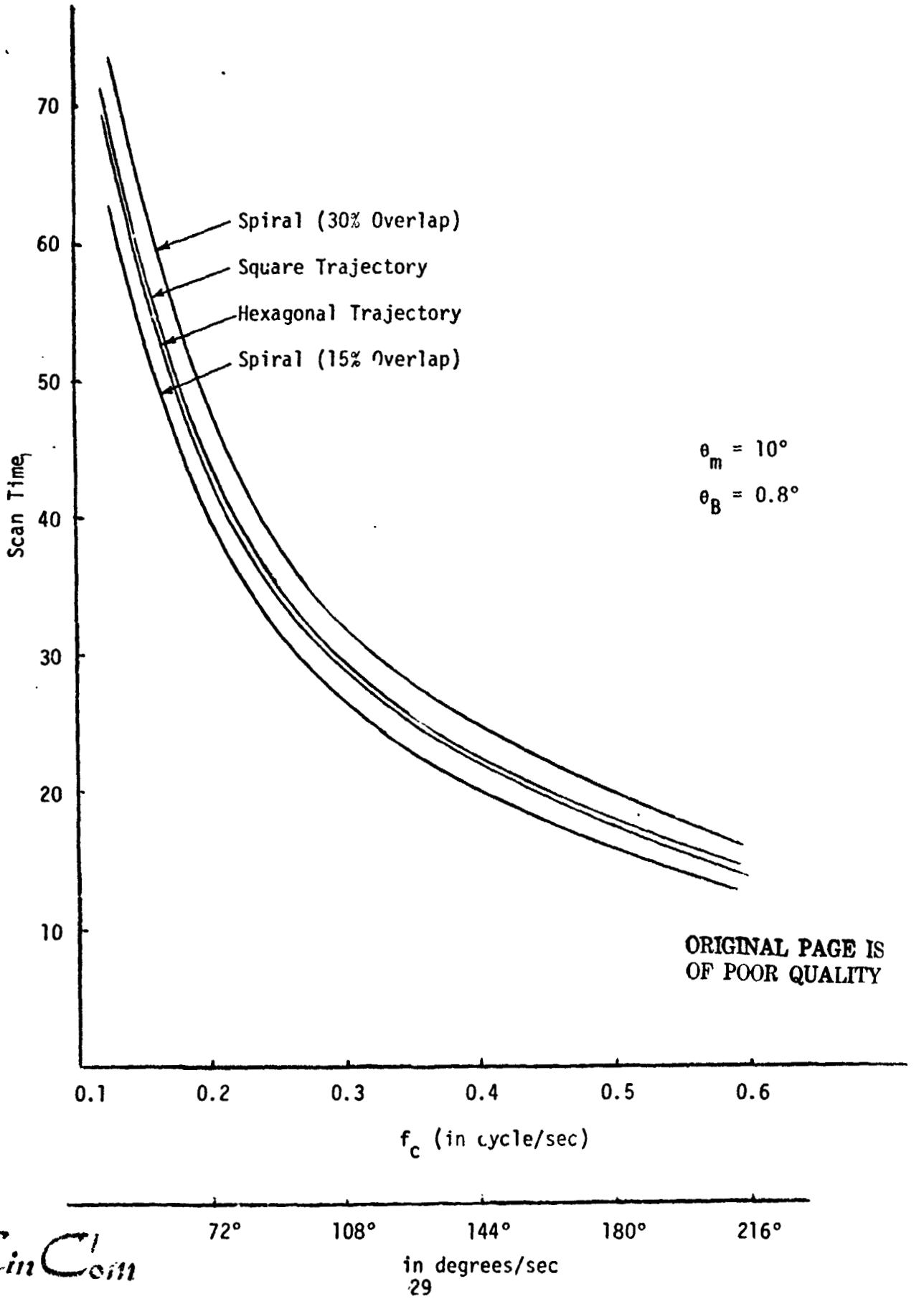

ORIGINAL PAGE IS
OF POOR QUALITY

per sec. The uncertainty cone is also assumed to be 20°. The curves show that the Shuttle antenna requires tc move 4.9°/sec along the spiral trajectory of 15% overlap to sweep over the whole uncertainty cone for 55 sec.

From Figs. 11 and 12, one can see that the scan time for spiral trajectory can be better than the other two trajectories. As pointed out previously, the square trajectories spend much more its scan beyond the uncertainty region. Similarly, the hexagonal trajectories may also spend some of its scan beyond the uncertainty region in order to ensure a complete coverage of the region. In general the path of trajectories starting from the center of uncertainty zone to its edge is shorter for spiral types than for square and hexagonal types. Therefore, the spiral trajectories are recommended for Shuttle antenna scanning.

Note that the constant speed along a trajectory yields a nonuniform angular velocity. In order to reveal the relation between the angular velocity and the constant speed along a trajectory, we plot the instantaneous angular velocity for a constant speed along a spiral trajectory, say 5°/sec, in Fig. 13. Clearly it shows that in the neighborhood of the center of the ucnertainty cone, the Shuttle antenna is required to rotate more than 4 cycles/sec, which may appear too high for the Ku-band receiver antenna. To prevent this situation, the combination of the constant angular velocity around the center of the uncertainty zone and the constant speed along a trajectory for

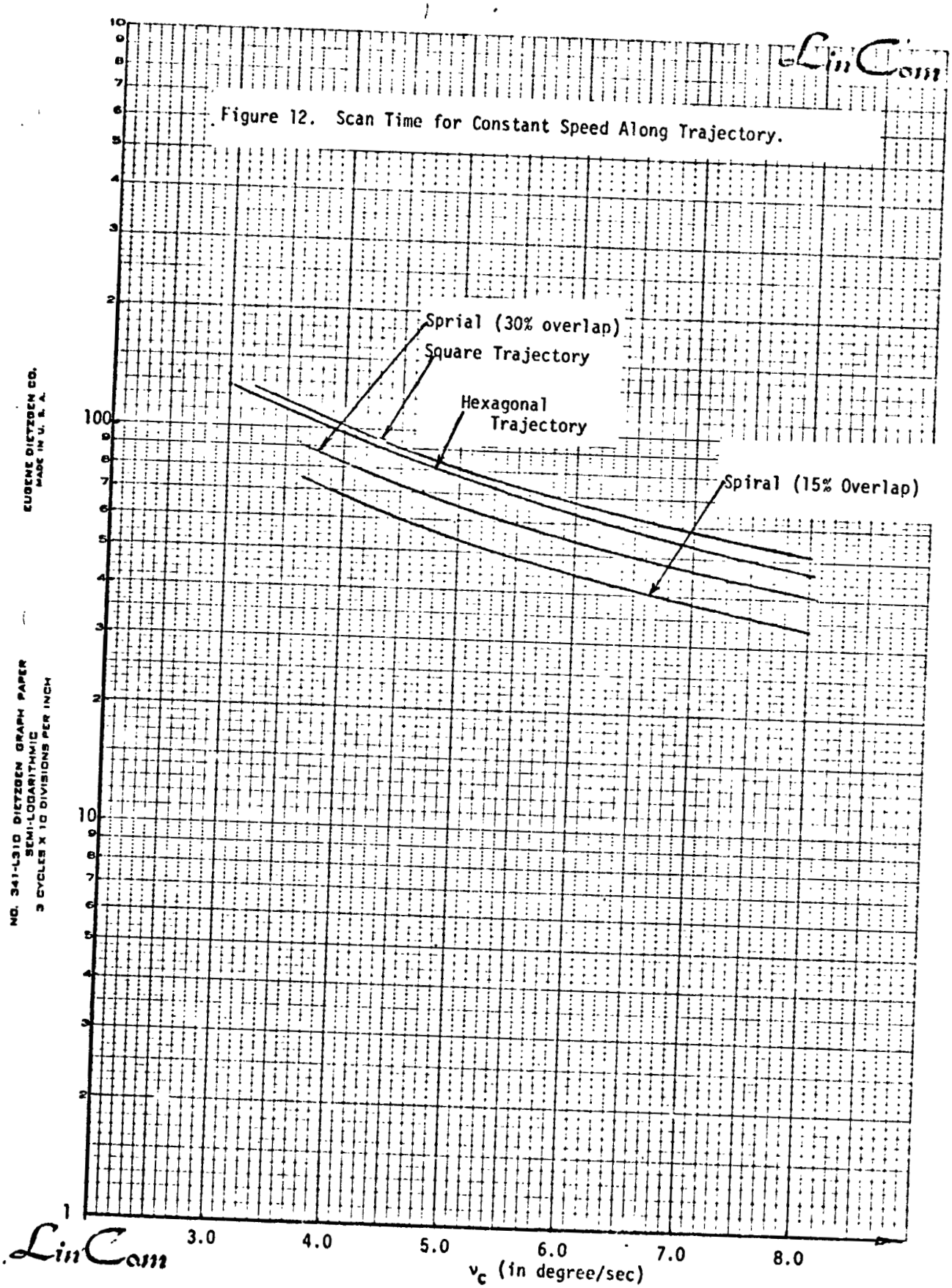

ORIGINAL PAGE IS OF POOR QUALITY

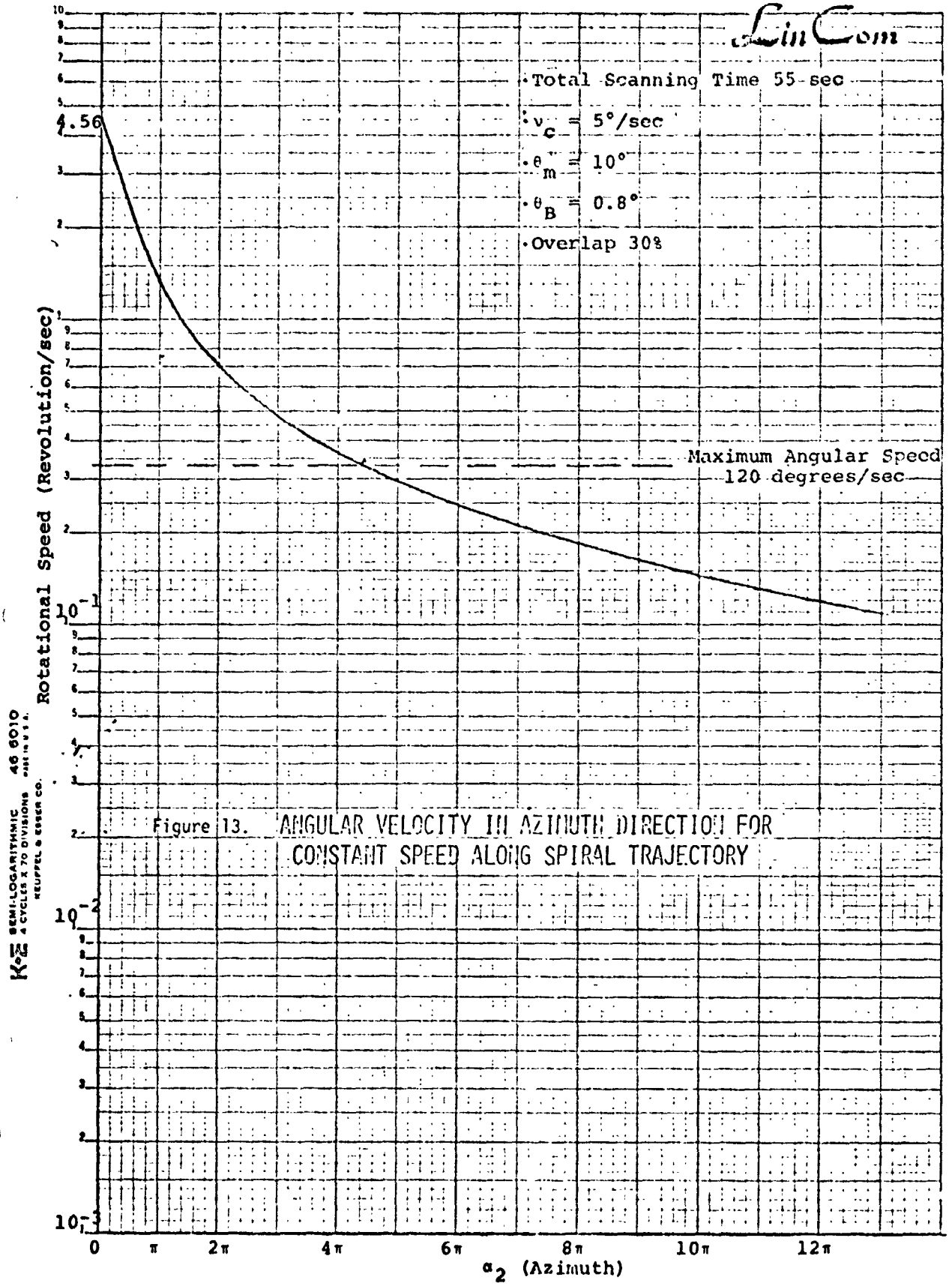

Figure 13. ANGULAR VELOCITY IN AZIMUTH DIRECTION FOR CONSTANT SPEED ALONG SPIRAL TRAJECTORY

outside area is proposed as the third alternative for the study.

For the third alternative, an additional parameter, called switch point θ_s, defining the point to change the motion of the Shuttle antenna from the constant angular speed to the constant speed along a trajectory, should be determined by the consideration of optimal dwell time for search cells. Here 'optimal' dwell time means to provide maximal available dwell time for signal detection. Thus, we shall discuss this problem in the next section.

(3) Dwell Time - Mechanical and Electrical

There are two kinds of dwell time involved in the acquisition system of spatial search--mechanical and electrical dwell times. The mechanical dwell time is defined to be the time interval for Shuttle antenna to sweep along a trajectory from one search cell to an adjacent cell; while the electrical dwell time is the time interval for a signal energy detector to integrate the received signal energy and making a decision. Surely the electrical dwell time governed by the mechanical dwell time. In this study, we assume that the electrical dwell time is much smaller than the mechanical dwell time and that the electrical dwell time will be set uniformly for all search cells. The relation between these two dwell times is given as follows:

$$T_D = k_D \min(T_{DM}) \tag{24}$$

where

T_{DM} = mechanical dwell time

T_D = electrical dwell time.

ORIGINAL PAGE IS OF POOR QUALITY

For a constant speed along trajectories, the mechanical dwell time is uniform. Eq. (16) becomes

$$T_D = k_D T_{DM} . \tag{24a'}$$

For a constant angular velocity, the mechanical dwell time varies depending on the location of cells. When the trajectory is near the center of the uncertainty zone, the number of cells swept by the Shuttle antenna per cycle is less and the mechanical dwell time is longer. Therefore, the shortest mechanical dwell time available occurs at the outward area of the uncertainty cone. One may estimate the shortest mechanical dwell time by

$$\min(T_{DM}) \approx \frac{1}{f} \frac{(\theta_B - \frac{\Delta}{2})}{\pi\theta_M} \tag{25}$$

where

θ_M = radius of uncertainty cone

$2\theta_B$ = beamwidth of antenna

f = revolution/sec

$\Delta/2\theta_B$ = overlap

Next we discuss the case where the Shuttle antenna moves with constant angular velocity around the center of the uncertainty area then changes to a constant speed along a trajectory at a switching point θ_s. We have plotted curves, as shown in Fig. 14, for $k_D = 0.1$, and fixed total scan time $T_{scan} = 55$ sec. When the switching point at $\theta_s = 6°$, the intersection of curves A and B yields the optimal electrical dwell time available, $T_D = 22.5$ ms if one chose $f_c = 0.26$ cycle/sec for rotational speed within the switching point θ_s. The curve A represents the minimum dwell time for cells within the constant rotation zone, while curve B is the dwell time of cells outside the constant rotation zone. Based on these sets of curves, a

Figure 14. Optimization of Electrical Dwell Time.

LinCom

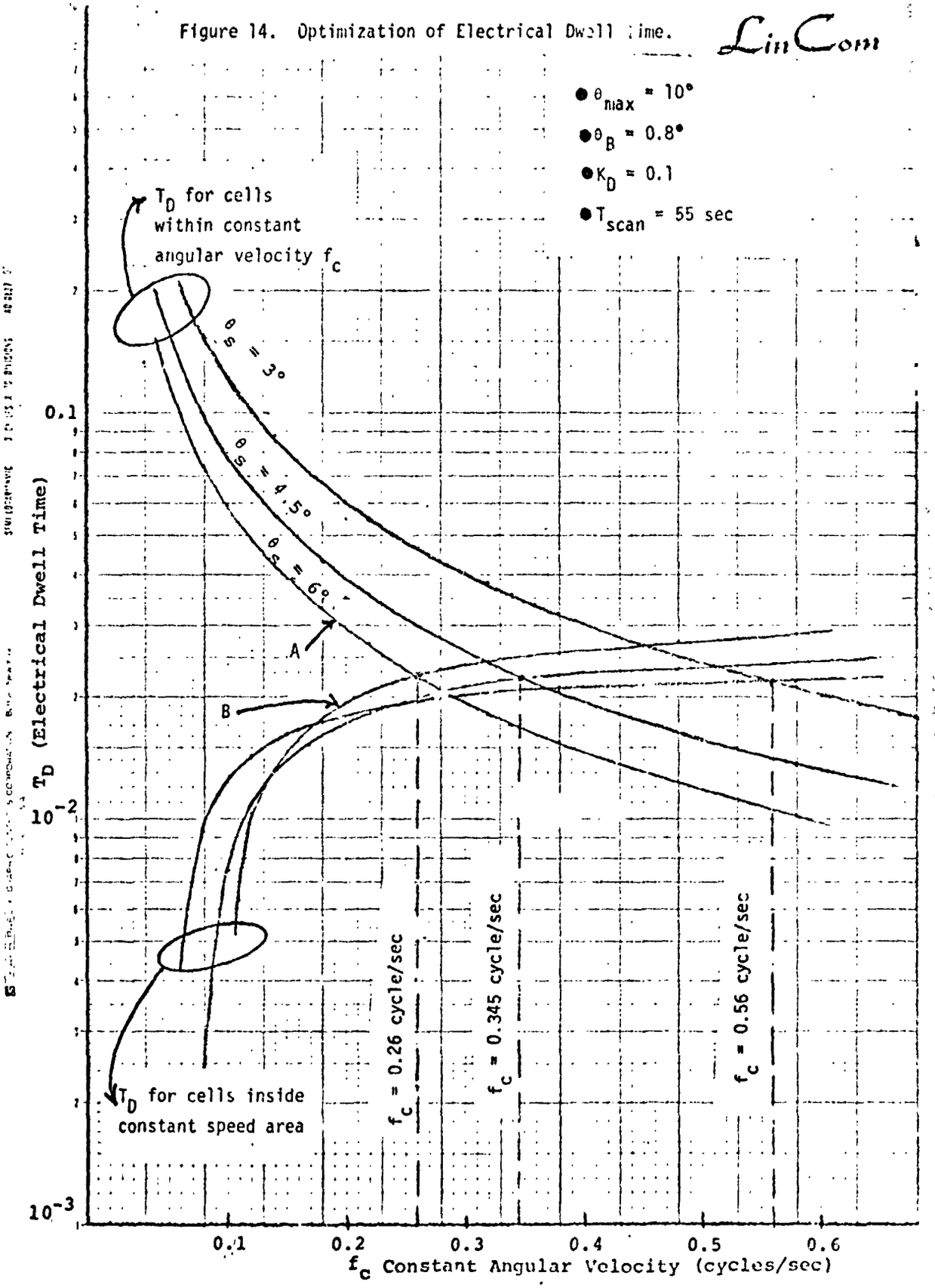

ORIGINAL PAGE IS
OF POOR QUALITY

system designer may determine the optimal electrical dwell time and also proper rotation speed. The constant speed for the outside switch point can be set to be the same speed as that when the Shuttle antenna reaches the switch point, that is

$$\left.\frac{ds}{dt}\right|_{\text{at } \theta_s} = \theta_s \left.\frac{d\alpha_2}{dt}\right|_{\text{at } \theta_s} = 2\pi f_c \theta_s. \qquad (26)$$

ORIGINAL PAGE IS
OF POOR QUALITY

III. AVERAGE SCAN TIME (MECHANICAL)

Scan time is one of the important parameters in the design of antenna acquisition systems. It is functions of the mechanical characteristtics of the Shuttle antenna, the scheme of signal energy detection and the statistical position of TDRS relative to Shuttle users. The analysis of the scan time is rather complicated. In this study, we shall resort to computer simulation to obtain the scan time. However, we shall discuss the scan time of the Shuttle antenna without taking into account the effects of false-alarm and miss detection. This means the scan time will be determined for a chosen antenna trajectory, type of motion of gimbol systems and truncated Gaussian distribution for the TDRS position.

To derive the average scan time for the Shuttle antenna to point to the TDRS position, we shall use Gauss quadrature rules, for which a general expression of scan time T conditioned on a known TDRS positions is required.

For the three proposed scanning trajectories the scan time T will be expressed in terms of either a rectangular coordinate system for spiral trajectories or in a rectangular coordinate system for two other trajectories--square and hexagonal.

Denote the TDRS position to be at $\hat{\alpha}$ $(\hat{\alpha}_{EL},\hat{\alpha}_{AZ})$, where $\hat{\alpha}_{EL}$ is in elevation component (radical direction in the projected plane) and $\hat{\alpha}_{AZ}$ is in azimuth component (angular direction). Let $x(t)$ and $y(t)$ be the rectangular coordinates of the trajectory of the Shuttle antenna motion on a projected plane at time instant t. One can relate it to the polar coordinates (α_1,α_2)

ORIGINAL PAGE IS
OF POOR QUALITY

as follows

$$\alpha_1(t) = \sqrt{x^2(t) + y^2(t)} \quad \text{in Elevation Direction} \tag{27}$$

$$\alpha_2(t) = \tan^{-1}\frac{x(t)}{y(t)} \quad \text{in Azimuth Direction} \tag{28}$$

In the analysis, it is assumed that, to start the spatial search of the TDRS position, the Shuttle antenna points to the designated center of the uncertainty region of TDRS, say $\alpha(t) = (0,0)$ as shown in Fig. 15. Then the time required for the Shuttle antenna to scan up to the TDRS position, along the assigned scanning trajectory can be expressed as follows:

$$T(\hat{\alpha}) = \int_{\alpha=0}^{\hat{\alpha}=\hat{\alpha}} dt = \int_{\alpha=0}^{\hat{\alpha}} \left(\frac{dt}{ds}\right) ds \quad \text{along trajectory } P_j \tag{29}$$

where P_j is the assigned trajectory of the Shuttle antenna motion, as seen in Fig. 15. The variable $\left(\frac{ds}{dt}\right)$ is the velocity of the antenna motion along the trajectory at any instant t. More often, it is rather convenient to decompose the speed of antenna motion into two orthogonal components, either in polar form or in rectangular form. From geometric considerations one can simply express $\left(\frac{ds}{dt}\right)$ in the following forms:

$$\left(\frac{ds}{dt}\right) = \sqrt{\left(\alpha_1 \frac{d\alpha_2}{dt}\right)^2 + \left(\frac{d\alpha_1}{dt}\right)^2} \quad \text{in Polar Form} \tag{30}$$

or

$$\frac{ds}{dt} = \sqrt{\left(\frac{dx}{dt}\right)^2 + \left(\frac{dy}{dt}\right)^2} \quad \text{in Rectangular Form} \tag{31}$$

Therefore the conditional scanning time $T(\hat{\alpha})$ on the known TDRS

Figure 15. ANTENNA TRAJECTORIES

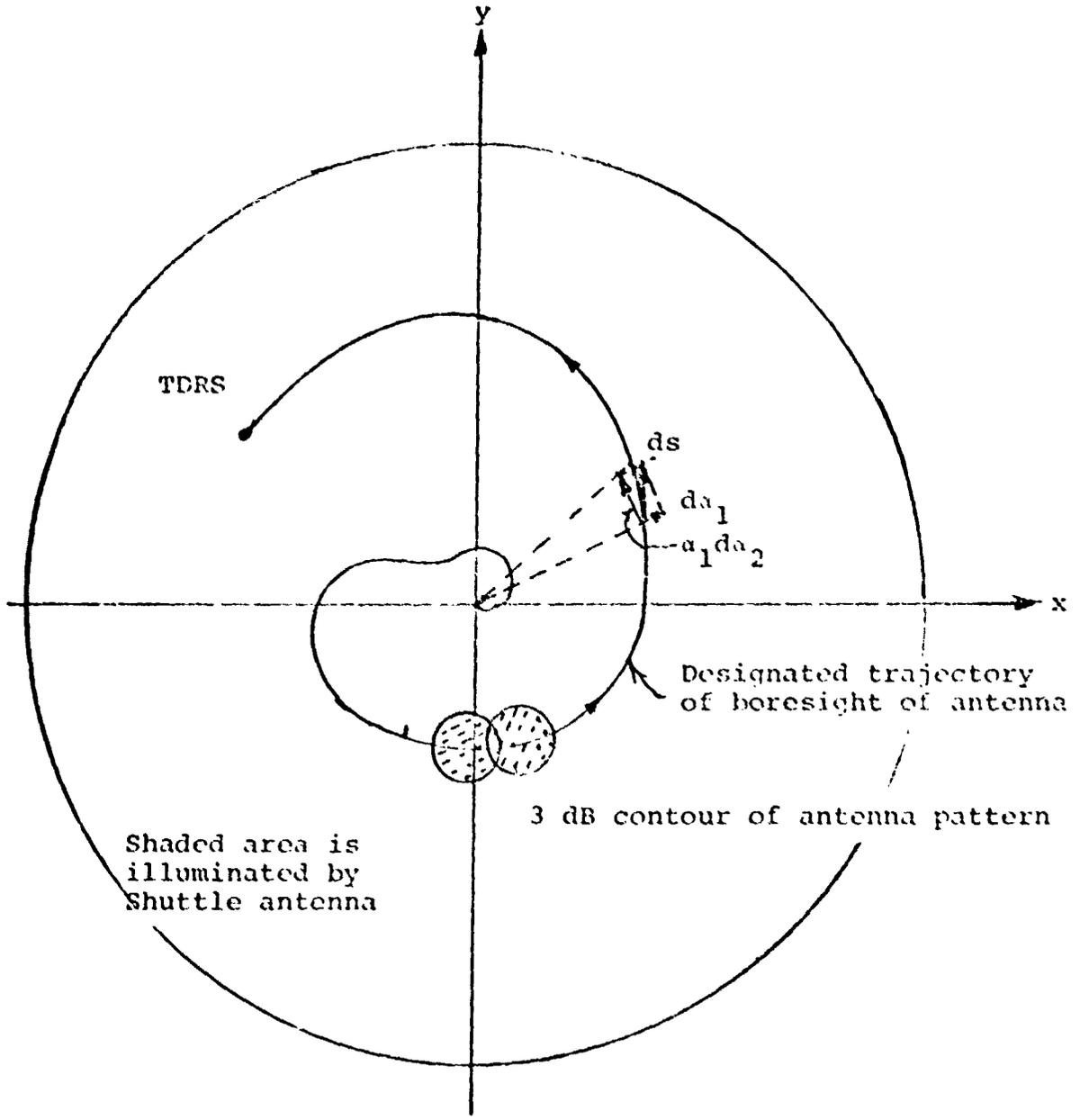

TRAJECTORY PROJECTED ONTO A PLANE PERPENDICULAR TO THE DIRECTION OF DESIGNATED CENTER OF UNCERTAINTY ZONE

position become

$$T(\hat{\alpha}) = \int_{\substack{\alpha=0 \\ \text{along } P_j}}^{\hat{\alpha}} \frac{ds}{\sqrt{\left(\alpha_1 \frac{d\alpha_2}{dt}\right)^2 + \left(\frac{d\alpha_1}{dt}\right)^2}} \quad \text{for Polar Form} \qquad (32a)$$

or

$$T(\hat{\alpha}) = \int_{\substack{(0,0) \\ \text{along } P_j}}^{(\hat{x},\hat{y})} \frac{ds}{\sqrt{\left(\frac{dx}{dt}\right)^2 + \left(\frac{dy}{dt}\right)^2}} \quad \text{for Rectangular Form} \qquad (32b)$$

One can evaluate the scan time using the above formulation if the trajectory is fixed and the TDRS position is known. Unfortunately, in practice the TDRS position is only known within a certain region. To characterize this unknown, a truncated Gaussian distribution function $p(\alpha_1,\alpha_2)$ is assumed for the TDRS position. That means $\hat{\alpha}$ is a random variable with probability distribution $p(\alpha_1,\alpha_2)$. With this uncertainty of the TDRS position, the average scan time can be evaluated through Gauss quadrature formulas. By definition, the average scan time is

$$\overline{T(\hat{\alpha})} = E_{\hat{\alpha}}[T(\hat{\alpha})]$$

$$= \iint T(\alpha_1\ \alpha_2)p(\alpha_1,\alpha_2)d\alpha_1\ d\alpha_2 \qquad (33)$$

Here we shall assume that the variables α_1 and α_2 are statistically independent of each other, as is the case in practice, i.e.

ORIGINAL PAGE I
OF POOR QUALITY

$$p(\alpha_1,\alpha_2) = p_1(\alpha_1)p_2(\alpha_2)$$

Then one has

$$\overline{T(\hat{\alpha})} = \int_0^{\theta_m} p_1(\alpha_1) \int_0^{2\pi} T(\alpha_1,\alpha_2)p_2(\alpha_2)d\alpha_2\, d\alpha_1$$

where

θ_m = the radius of the uncertainty region of TDRS position

The above double integral can be evaluated approximately through Gauss quadrature formulas as below:

$$\overline{T} = \sum_{\ell=1}^{N_1} \sum_{k=1}^{N_2} \omega_{1\ell}\omega_{2k}T(\alpha_{1\ell},\alpha_{2k}) \qquad (34)$$

The sets of parameters $(\omega_{1\ell},\alpha_{1\ell})$ and $(\omega_{2k},\alpha_{2k})$ can be obtained from moments of random variables. A set of these parameters for the assumed probability distribution function (as shown in previous sections that the random variable α_1 is truncated Rician distribution and α_2 uniform distribution) is given in Table 1 for $N_1 = N_2 = 5$ with required moments of random variables.

Through this scheme, the average scan time with two different types of the antenna motion along spiral trajectory of 30% overlap is computed vs σ_p, the standard deviation of the Gaussian distribution function The Shuttle antenna will take 31.5 sec to sweep over the whole uncertainty area if it is rotated with a constant angular velocity of 0.3 cycle/sec. The average scan time for this constant angular velocity is plotted in Fig. 16. For a mixed type of motion--sweeping with a constant angular velocity f_c then constant speed along the trajectory v_c at a switching angle θ

Table I. Moments and Parameters ($\omega_{i\ell}, \alpha_{i\ell}$) of Gauss Quadrature Formulas.

(1) Truncated Rician Variable ($\theta_m = 1.0°, \sigma_p = 0.25°$)

	(I-1)TH Central Moments
1	1.0000000E+00
2	3.1307825E-01 (Mean)
3	2.6646434E-02
4	2.6520391E-03
5	2.2308420E-03
6	6.2739134E-04
7	3.5791496E-04
8	1.5581140E-04
9	8.4715485E-05
10	4.4132538E-05
11	2.4764277E-05

Gauss Quadrature Formula

	$\alpha_{1\ell}$	$\omega_{1\ell}$
0	-2.4194992E-01	1.2466771E-01
1	-9.5548526E-02	4.1508332E-01
2	9.9011891E-02	3.6030230E-01
3	3.2591406E-01	9.3469248E-02
4	5.6917592E-01	6.4774140E-03

(2) Uniform Random Variable ($\theta_m = 1.0$)

	(I-1)TH Central Moment
1	1.0000000E+00
2	5.0000000E-01 (Mean)
3	8.3333333E-02
4	0.
5	1.2500000E-02
6	0.
7	2.2321429E-03
8	0.
9	4.3402778E-04
10	0.
11	8.8778409E-05

Gauss Quadrature Formula

	$\alpha_{2\ell}$	$\omega_{2\ell}$
0	-4.5308993E-01	1.1846344E-01
1	-2.6923466E-01	2.3931434E-01
2	-7.9936058E-14	2.844444E-01
3	2.6923466E-01	2.3931434E-01
4	4.5308993E-01	1.1846344E-01

LinCom

Figure 16. AVERAGE SCAN TIME FOR CONSTANT ANGULAR VELOCITY

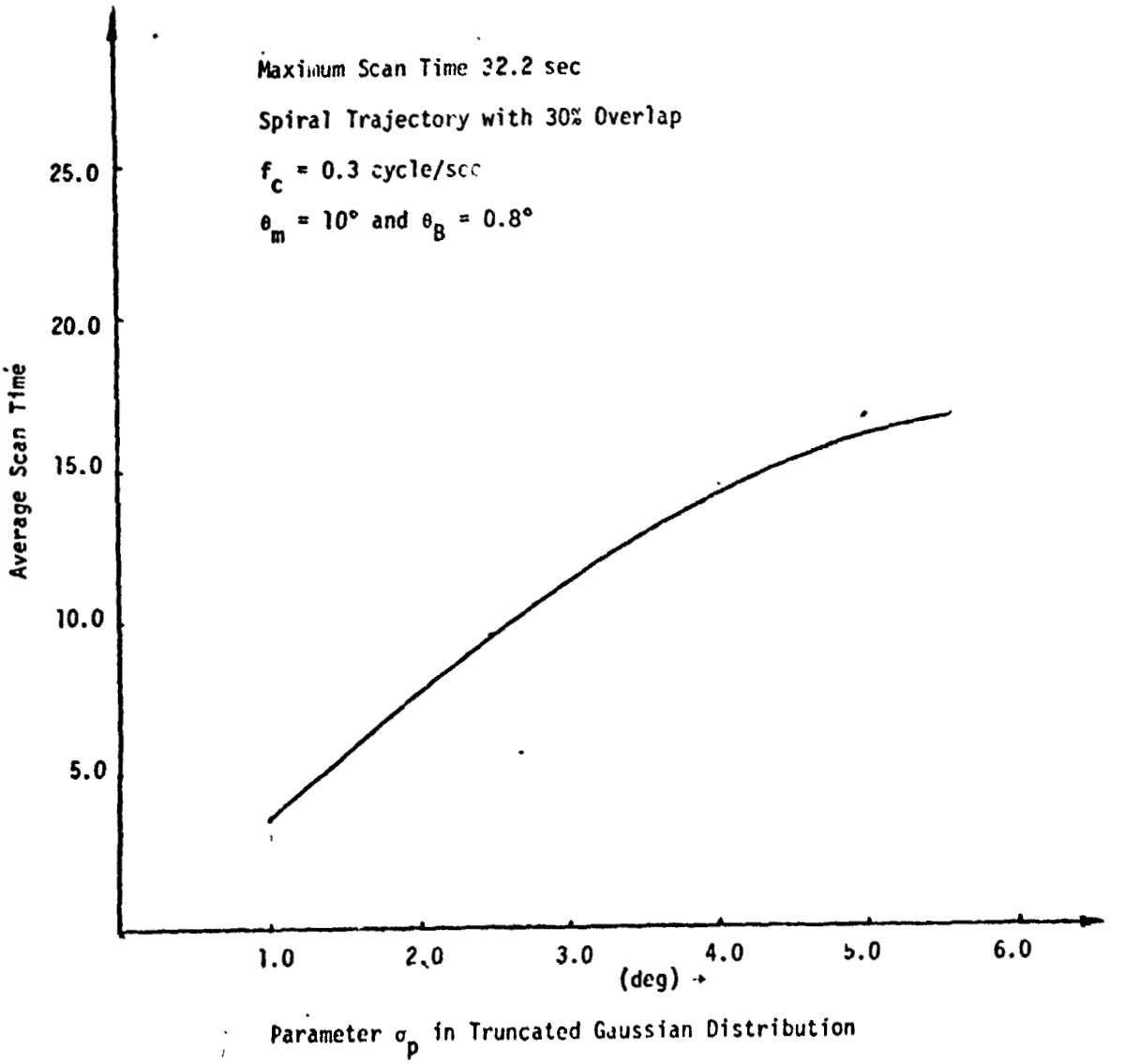

LinCom

the Shuttle antenna will take 61.6 sec to complete the scan over the uncertainty area if f_c = 0.3 cycle/sec, ν_c = 5 044 degrees/sec. Its average scan time is also plotted in Fig. 17. Note that the unit of ν_c is the same as that in elevation unit/sec.

ORIGINAL PAGE IS
OF POOR QUALITY

Figure 17. AVERAGE SCAN TIME FOR A MIXED MOTION

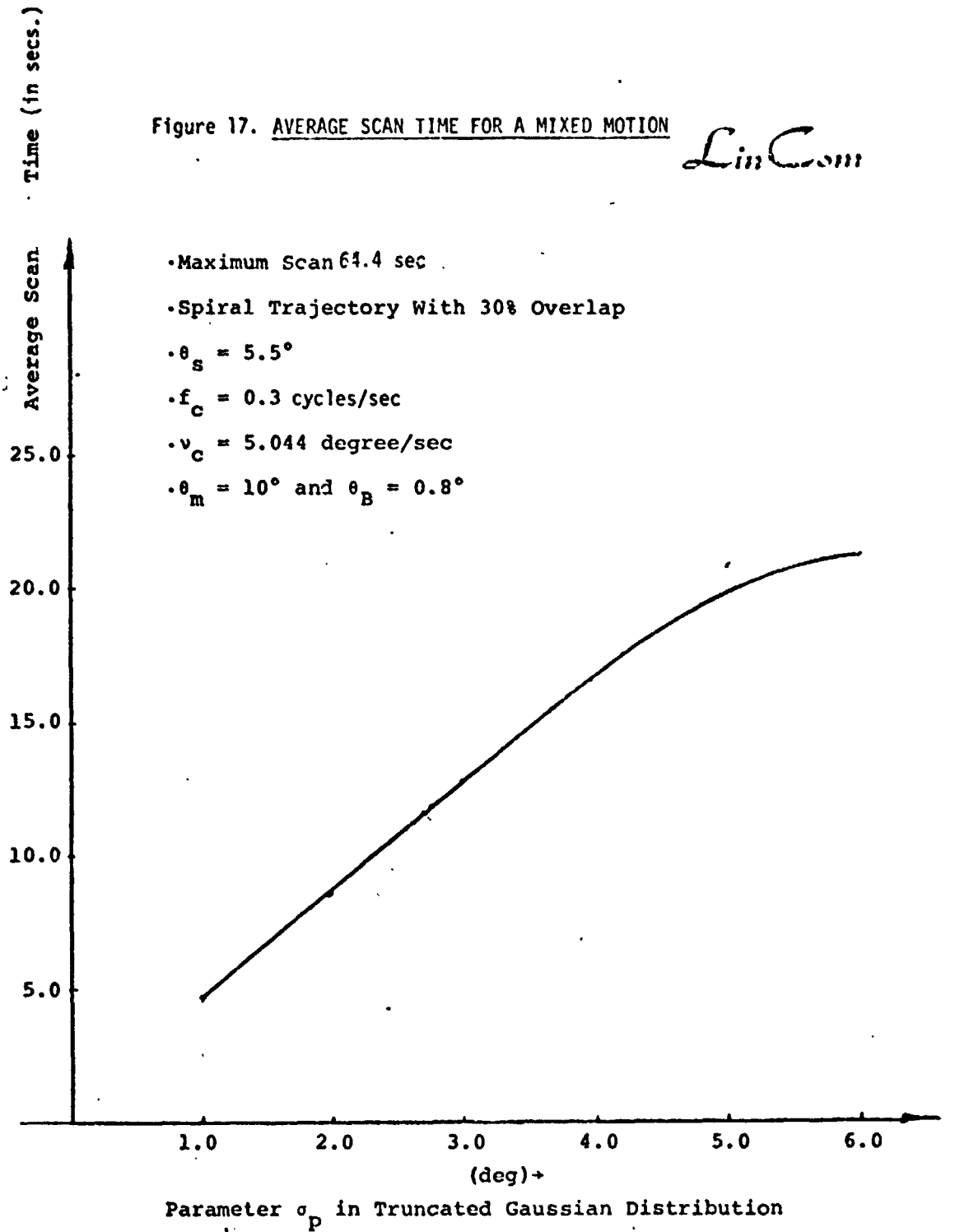

IV. KU-BAND RECEIVER--SIGNAL ENERGY DETECTOR

(1) Receiver Model

In this study tne receiver for spatial search is assumed to be a noncoherent signal energy detector, as shown in Fig. 19. The signal energy from a square-law detector is used for detecting whether the Shuttle antenna is pointing toward the TDRS. During the spatial search, the Shuttle antenna is sweeping across the uncertainty region of the TDRS along the assigned trajectory. At the same time the Shuttle receives signals transmitted from the TDRS. The signal power received by the Shuttle depends upon the offset angle θ_{off} between the boresight axis of the Shuttle antenna and the direction of the TDRS in the view of the Shuttle receiver. By comparing the received signal power with a threshold, one can determine that the boresight axis of the Shuttle antenna is pointing to the TDRS, therefore, stops the scanning of the Shuttle antenna. Denote the received signal to be $S(t,\theta)$ plus the channel Gaussian noise with zero mean and variance σ_n^2. The received signal may be expressed as follows:

$$r(t,\theta) = S(t,\theta) + n(t) \tag{35}$$

where

$S(t,\theta) = \sqrt{2P}\, G(\theta)\, S_q(t) d(t) \cos \Phi(t)$

P = Maximum received signal power when the boresight of the Shuttle antenna is pointing at the TDRS position

$S_q(t)$ = PN code waveform

$d(t)$ = Data waveform

$\Phi(t) = \omega_0 t + \psi_0$

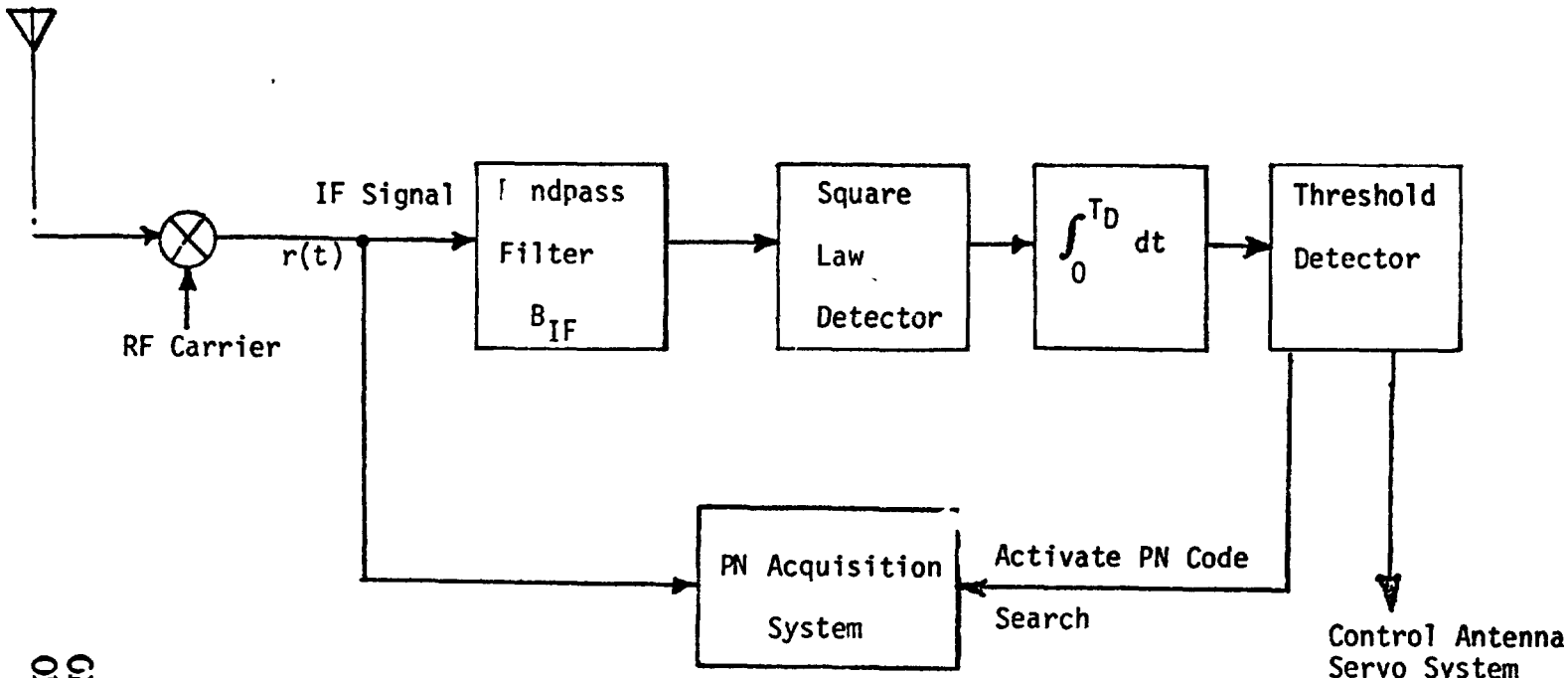

Figure 19. Signal Energy Detection for Spatial Search.

ORIGINAL PAGE IS
OF POOR QUALITY

$\frac{\omega_0}{2\pi}$ = Carrier frequency

ψ_0 = Initial phase angle

$G(\theta)$ = Loss function of received signal due to offset of the boresight of the Shuttle antenna from the TDRS position as defined in eq. (8)

$n(t)$ = A Gaussian random process with zero mean and variance σ_n^2

$= n_c \cos \phi(t) - n_s \sin \phi(t)$

n_c, n_s = Baseband Gaussian random processes with zero means and variances σ_n^2

The variance σ_n^2 of the channel noise is determined by the bandwidth of the IF filter B_{IF} and system noise temperature (noise spectral density N_0). Since the received signal is wide spread in frequency, the IF filter must be designed to be wide enough to pass the signal. Therefore, the received signal power consists of not only the transmitted signal energy but also channel noise energy. When the available signal power at the Shuttle receiver is weak, the decision making based on the output of energy detection will be effected by the channel noise power; however, one can set proper threshold against the channel noise so that the probability of detecting $\theta_{eff} = 0$ is reasonably high. Yet, when the available signal power is strong, the criterion of setting threshold level against the channel noise will cause false acquisition due to sidelobe of the Shuttle antenna, since the sidelobe of the Shuttle antenna is only 17 dB weaker than the strength of the main lobe of the antenna. In order to prevent this sidelobe acquisition, special

schemes must be implemented. Some recommended techniques for avoidance of sidelobe acquisition will be discussed separately.

The signal detection for the Ku-band receiver can be formulated as follows:

Denote the output of the square law detector to be

$$y(t,\theta) = r^2(t,\theta) \tag{36}$$

depending on the offset angle between the boresight axis of the Shuttle antenna and the direction of the TDRS. The output of the integrator is

$$Z(\theta) = \frac{1}{T_D} \int_0^{T_D} r^2(t,\theta)dt \tag{37}$$

The detector is to determine one of two hypotheses:

$$\begin{aligned} H_0&: \ Z(\theta) \qquad |\theta| \geq \theta_a \\ H_1&: \ Z(\theta) \qquad |\theta| < \theta_a \end{aligned} \tag{38}$$

where θ_a= allowable offset angle of the Shuttle antenna. The integration of $Z(\theta)$ will be approximated by the sum of N samples taken at a Nyquist rate T_s, which is equal to B_{IF}^{-1}.

$$Z(\theta) = \frac{1}{M} \sum_{n=1}^{M} r^2(kT_s,\theta) \tag{39}$$

where M = integer part of $B_{IF}T_D$. The statistical characteristics of the variable $Z(\theta)$ can be determined from that of a single sample $r(kT_s,\theta)$, to be discussed in the next section. Here we shall further make one assumption that $\theta_a \approx 0$. So the hypotheses should be modified as

$$H_0: \ Z(\theta) \qquad \text{for } |\theta| > 0$$
$$H_1: \ Z(\theta) \qquad \text{for } \theta = 0 \tag{40}$$

The following analysis can be modified for small values of θ_a.

(2) Statistical Characteristics of Decision Variable

By the assumption that n_c and n_s are two lowpass Gaussian random variables of zero means and variance σ_n^2, the probability density function of the envelope R and phase ψ of the signal $r(t,\theta)$ is well known

$$P(R,\psi|\theta,S_q,d) = \begin{cases} \dfrac{R}{2\pi\sigma_n^2} \exp\left(\dfrac{2PG^2(\theta) + R^2 - 2\sqrt{2P}G(\theta)S_q(t)d(t)R\cos\psi}{-2\sigma_n^2}\right) & \text{for } R \geq 0 \\ 0 \qquad \text{for } R < 0 \end{cases} \tag{41}$$

where

$$R = [\sqrt{2P}G(\theta)S_q(t)d(t)+n_c]^2 + n_s^2$$

$$\psi = \tan^{-1} \frac{n_s}{\sqrt{2P}G(\theta)S_q(t)d(t) + n_c}$$

ORIGINAL PAGE IS
OF POOR QUALITY

Define

$$\rho^2(\theta) = \frac{PG^2(\theta)}{\sigma_n^2} = \text{input signal-to-noise ratio (SNR)}$$

Then

$$P(R,\psi|\theta,S_q,d) = \begin{cases} \dfrac{R}{2\pi\sigma^2} \exp\left(-\left(\dfrac{R}{\sqrt{2}\sigma_n}\right)^2 - \rho^2(\theta) + 2\rho(\theta)\left(\dfrac{R}{\sqrt{2}\sigma_n}\right)S_q(t)d(t)\cos\psi\right) & \text{for } R \geq 0 \\ 0 \qquad R < 0 \end{cases} \tag{42}$$

Averaging $P(R,\psi|\theta)$ with respect to ψ, one has

$$P(R|\theta,S_q,d) = \begin{cases} \frac{R}{\sigma_n^2} \exp\left(-\left(\frac{R}{\sqrt{2}\sigma_n}\right)^2 - \rho^2(\theta)\right) I_0\left(\frac{R}{\sqrt{2}\sigma_n} S_q(t)d(t)\rho(\theta)\right) & R > 0 \\ 0 & R < 0 \end{cases} \quad (43)$$

Assuming that

$$S_q(t) = \left\{ \begin{matrix} +1 \\ -1 \end{matrix} \right\} \quad \text{with equal probabilities}$$

and

$$d(t) = \left\{ \begin{matrix} +1 \\ -1 \end{matrix} \right\} \quad \text{with equal probabilities}$$

then one has

$$P(r_\ell|\theta) = \begin{cases} \frac{r_\ell}{\sigma_n^2}\left(\exp\left(-\frac{r_\ell}{\sqrt{2}\sigma_n}\right)^2 - \rho^2(\theta)\right) I_0\left(\left(\frac{r_\ell}{\sqrt{2}\sigma_n}\right)\rho(\theta)\right) & \text{for } r_\ell > 0 \\ 0 & \text{for } r_\ell < 0 \end{cases} \quad (44)$$

where

r_ℓ = sample of R at $t = \ell T_s$

ORIGINAL PAGE IS
OF POOR QUALITY

Now we can derive the probability density function of $Z(\theta)$ from $P(r_\ell|\theta)$ through the characteristic function approach, which can be found in [1]. Omitting the detailed derivation, we express the result as

$$P(Z|\theta) = \begin{cases} \frac{M}{2\sigma_n^2}\left(\frac{Z}{2\sigma_n^2\rho^2(\theta)}\right)^{M-1/2} \exp\left(-\frac{MZ}{2\sigma_n^2} - M\rho^2(\theta)\right) \\ \qquad I_{M-1}\left(2M\rho(\theta)\sqrt{\frac{Z}{2\sigma_n^2}}\right) & \text{for } z \geq 0 \\ 0 & Z < 0 \end{cases} \quad (45)$$

where

$I_{M-1}(\cdot)$ = Modified Bessel function of the first kind and of order (M-1).

(3) Probability of Detection and False Alarm

When $\theta = 0$, the probability of detecting the presence of TDRS can be computed as

$$P_d(\theta=0) = \int_{Th}^{\infty} P\{Z|\theta=0\}dZ$$

$$= \int_{TH}^{\infty} \frac{M}{2\sigma_n^2} \left(\frac{Z}{2\sigma_n^2\rho^2(0)}\right)^{M-1/2} \exp\left(-\frac{MZ}{2\sigma_n^2} - M\rho^2(0)\right) I_{M-1}\left(2M\rho(0)\sqrt{\frac{Z}{2\sigma_n^2}}\right) dZ \qquad (46)$$

where Th is a threshold level of the detection. Defining $Z_1 = MZ/2\sigma_n^2$, one has

$$P_d(\theta=0) = Q_M\left(M\rho^2(0), \frac{MTh}{2\sigma_n^2}\right) \qquad (47)$$

where

$$Q_M(x,y) = \int_y^{\infty} \left(\frac{z}{x}\right)^{M-1/2} \exp(-z-x) I_{M-1}(2\sqrt{xz})dz$$

The function $Q_M(x,y)$ is known as generalized Marcum's Q-function.

When the offset angle θ is nonzero ($\geq \theta_B$), the probability of false alarm can be expressed as

$$P_{fa}(\theta\neq 0) = \int_{Th}^{\infty} P(Z|\theta\neq 0)dZ$$

$$= Q_M\left(M\rho^2(\theta), \frac{MTh}{2\sigma_n^2}\right) \qquad (48)$$

ORIGINAL PAGE IS OF POOR QUALITY

which is a function of the offset angle θ. The criterion for choosing Th is the prevention of false detection caused by the second sidelobe of the Shuttle antenna. In practice, for a given false alarm probability, one needs to establish the threshold level Th. However, solving for Th from eq. (48) for a given value of $P_{fa}(\theta)$ appears to be nontrivial unless some approximation is made. Thus one may assume that $\rho^2(\theta \neq 0) \approx 0$.

$$P_{fa}(\theta \neq 0) = \lim_{\rho^2(\theta \neq 0) \to 0} Q_M\left(M\rho^2(\theta), \frac{MTh}{2\sigma_n^2}\right)$$

$$= \frac{1}{\Gamma(M)} \int_{\frac{MTh}{2\sigma_n^2}}^{\infty} Z^{M-1} \exp(-Z)dZ$$

$$= \left(\frac{MTh}{2\sigma_n^2}\right)^{M-1} \exp\left(-\frac{MTh}{2\sigma_n^2}\right) \sum_{k=0}^{M-1} \frac{1}{(M-k-1)!\left(\frac{MTh}{2\sigma_n^2}\right)^k}$$

for $M \geq 1$ (49)

Using iterative scheme one can solve for Th for a given value $P_{fa}(\theta \neq 0)$. In fact the above expression can be rewritten as

$$P_f(\theta \neq 0) = 1 - I\left(\sqrt{M\left(\frac{Th}{2\sigma_n^2}\right)}, M-1\right) \qquad (50)$$

where

$I(u,s)$ = incomplete gamma function

$$= \int_0^{u\sqrt{1+s^2}} \frac{x^s \exp(-x)}{s!} dx$$

The function $I(u,s)$ has been tabulated*. Thus one may

*Pearson, K., Tables of Incomplete Γ Function, Cambridge University Press, 1934.

conveniently solve for the threshold Th. Note that the approximation $\rho^2(\theta \neq 0) \approx 0$ is valid when the noise variance σ_n^2 is of the order of the first sidelobe magnitude (about SNR < 17 dB). Otherwise, alternative approximation may be taken. When signal-to-noise ratio SNR is high and the value of M is large, we shall use an equivalent Gaussian distribution for $P(Z|\theta)$.

$$P(Z|\theta) = \frac{1}{\sqrt{2\pi}\,\sigma_Z(\theta)} \exp\left(-\frac{(Z-m_Z(\theta))^2}{2\sigma_Z(\theta)}\right) \qquad (51)$$

where

$$m_Z(\theta) = M(1 + \rho^2(\theta)) \qquad (52a)$$

$$\sigma_Z^2(\theta) = M(1 + 2\rho^2(\theta)) \qquad (52b)$$

Then the probability of false alarm can be simply expressed as

$$P_f(\theta \neq 0) = \frac{1}{2}\,\mathrm{erfc}\left(\frac{\frac{M\,Th}{2\sigma_n^2} - m_Z(\theta)}{\sqrt{2}\,\sigma_n(\theta)}\right) \qquad (53)$$

where

$$\mathrm{erfc}(x) = \frac{2}{\sqrt{\pi}} \int_x^\infty \exp(-t^2)dt$$

Thus the threshold Th becomes

$$Th = \{\sqrt{2}\sigma_Z(\theta)\Phi^{-1}(P_f) + m_Z(\theta)\} * 2\sigma_n^2/M \qquad (54)$$

To evaluate Th, we substitute θ by θ_{sp}, the offset angle at which the first sidelobe of the antenna is located. The function $\Phi^{-1}(\cdot)$ is tne inverse function of erfc$(\cdot)$ function.

(4) Threshold Levels of Signal Energy Detector

The choice of threshold level in signal energy detection

depends upon the specification of false alarm probability and probability of detection and carrier-to-noise (CNR) ratio. One may start to choose initially a threshold Th_1 to meet the probability of false alarm P_{fa} due to channel noise. When CNR becomes larger, as indicated previously, one has to verify the chance of being acquiring the TDRS with the sidelobes of Shuttle antenna. If it is higher than P_{fa}, one needs to adjust the threshold level higher so that the probability P_{fas} of detecting the TDRS with sidelobe of antenna is less than specs.

However, in practice the CNR is not known at a Shuttle receiver, it is better for hardware implementation that a uniform threshold level for all operating range of CNR is set up. For a Ku-band communication link, the operating range of CNR can be as low as 60dB-Hz and as high as 80dB-Hz. With this wide range of CNR, (60 dB Hz - 80 dB Hz) one will find it impossible to set a uniform threshold level without having false acquisition due to sidelobe of the Shuttle antenna. This can be clearly seen when the signal energy at the output of detector is plotted for the main lobe against the sidelobe of Shuttle antenna, as shown in Fig. 19. Note that the signal energy received by a sidelobe of Shuttle antennas at CNR = 80 dB-Hz, can be stronger than the signal energy received by the main lobe of the antenna at CNR = 60 dB-Hz. Therefore, the threshold set up for CNR = 60 dB-Hz will be crossed by the signal energy of the sidelobe at CNR = 80 dB-Hz.

In order to avoid the false acquisition due to the sidelobe of the Shuttle antenna, a second threshold should be used to

Figure 19. Received Signal Energy.

LinCom

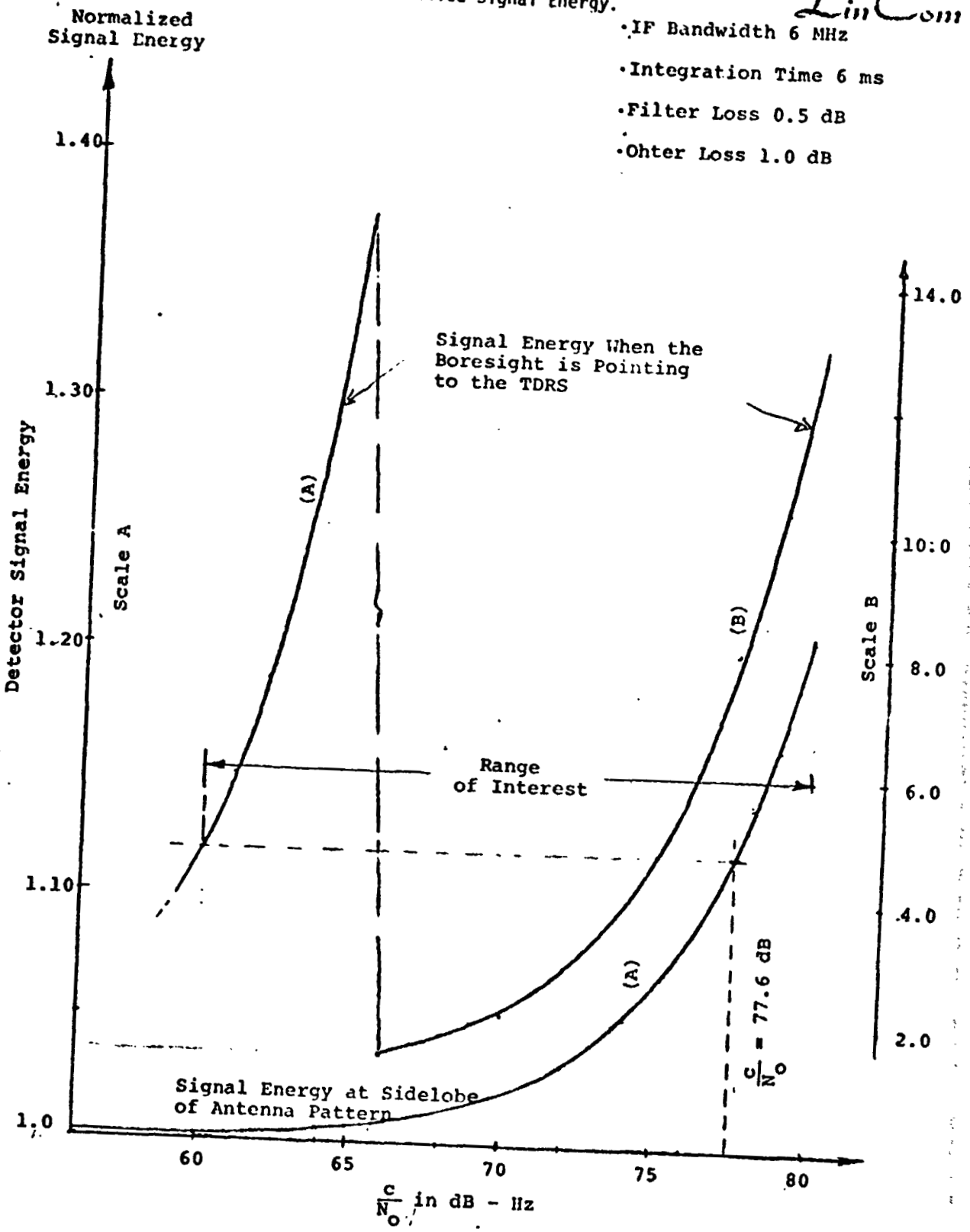

ORIGINAL PAGE IS
OF POOR QUALITY

distinguish the main lobe acquisition from a first sidelobe acquisition. Here it is proposed to use the second threshold level at CNR = 80 dB-Hz to guarantee the specs of the probability of false alarm due to the sidelobe for high SNR.

One also should note that for a wide operating range of CNR (60 dB-Hz to 80 dB-Hz), the possibility of having a second sidelobe acquisition occurs if the second sidelobe of antenna pattern is not lower than the main lobe by about the range of CNR.

V. ACQUISITION SYSTEM OF KU-BAND RECEIVER

1. Three Acquisition Strategies Studied

The acquisition system proposed for Ku-band receivers consists of two major parts--coarse spatial acquisition and autotrack acquisition. Here, we shall confine ourselves to the study of coarse spatial acquisition system. From the system point of view, it is expected that at the end of coarse acquisition, the boresight axis of the Shuttle antenna must be at least aligned with the direction of the TDRS position to within the pull-in range of the autotrack system. Three acquisition algorithms studied here can all acquire the TDRS within the main lobe of the Shuttle antenna when the received CNR at the receiver is not too high ($\leq$ 75 dB-Hz). However, with a wide dynamic range of CNR, one can identify the acquisition ranges of these three schemes to be within sidelobes of the Shuttle antenna, within the nulls of the main lobe and near 3 dB beamwidth of the antenna, respectively.

The acquisition schemes used for the coarse spatial search can be described as below:

(1) Normal scan - The boresight axis of the Shuttle antenna is offset at most from the direction of the TDRS position by an angle equal to the range of the first sidelobes of antennas. In this case the hit declared by the acquisition system may be due to either the main lobe or the first sidelobe of the antenna and this is dependent on the signal-to-noise ratio. Thus the autotrack system should be initiated to search for the TDRS position

by the main lobe of the Shuttle antenna.

(2) Normal scan plus the avoidance of the sidelobe acquisition- The scan will put the boresight axis of the Shuttle antenna within null angle of the main-lobe of the antenna from the TDRS position. For this case, the acquisition procedure is ended at the acquisition of the TDRS position with the mainlobe of the antenna. Thus the range of the autotrack operation will be much smaller than the previous case.

(3) Normal scan plus fine-search - At the end of the acquisition, the boresight axis of the Shuttle antenna will be within 3 dB beamwidth of the antenna from the TDRS position. This scheme shall not only avoid the sidelobe acquisition but also give a finer range for the autotrack acquisition. Surely the acquisition strategy for this case is much more complicated than the previous cases.

2. Acquisition Strategies

The acquisition strategies for the three acquisition schemes are depicted by flow diagrams in Figs. 20 , 21 and 22 , respectively. For the normal scan, there are only two stages within the acquisition--routine scan and verification. While the Shuttle antenna sweeps through the whole uncertainty area along a designated trajectory, the received signal energy at the output of the signal detector is compared against a preset threshold TH1. If the threshold is not exceeded, the search continues until the end of the whole area. If this is the case, the search fails to acquire and the search should restart.

Figure 20. Acquisition Strategy with Normal Scan.

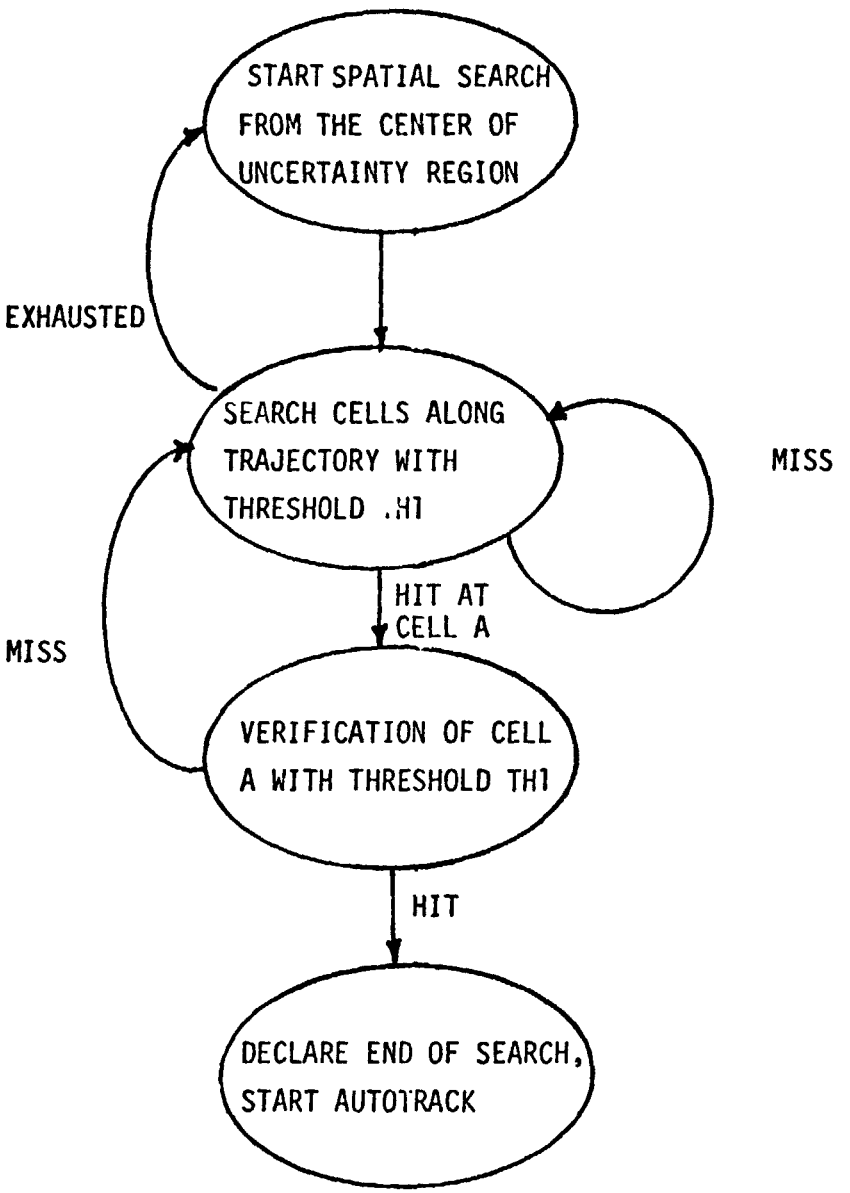

ORIGINAL PAGE IS
OF POOR QUALITY

Figure 21. Acquisition Strategy with Normal Scan Plus Sidelobe Scan.

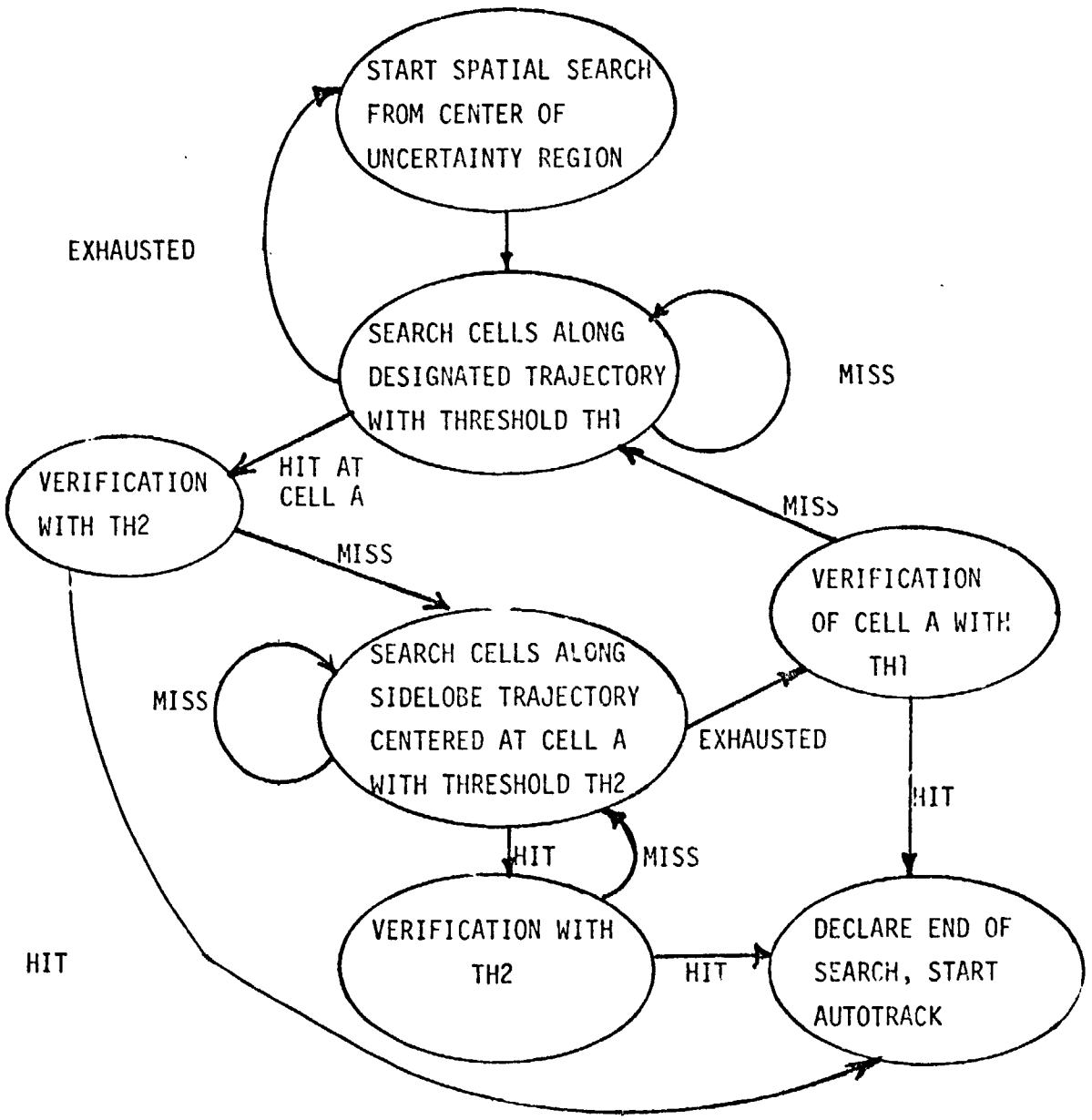

Figure 22. Acquisition Strategy with Normal Scan Plus Mini-Scans (Adjacent and Sidelobe Scans)

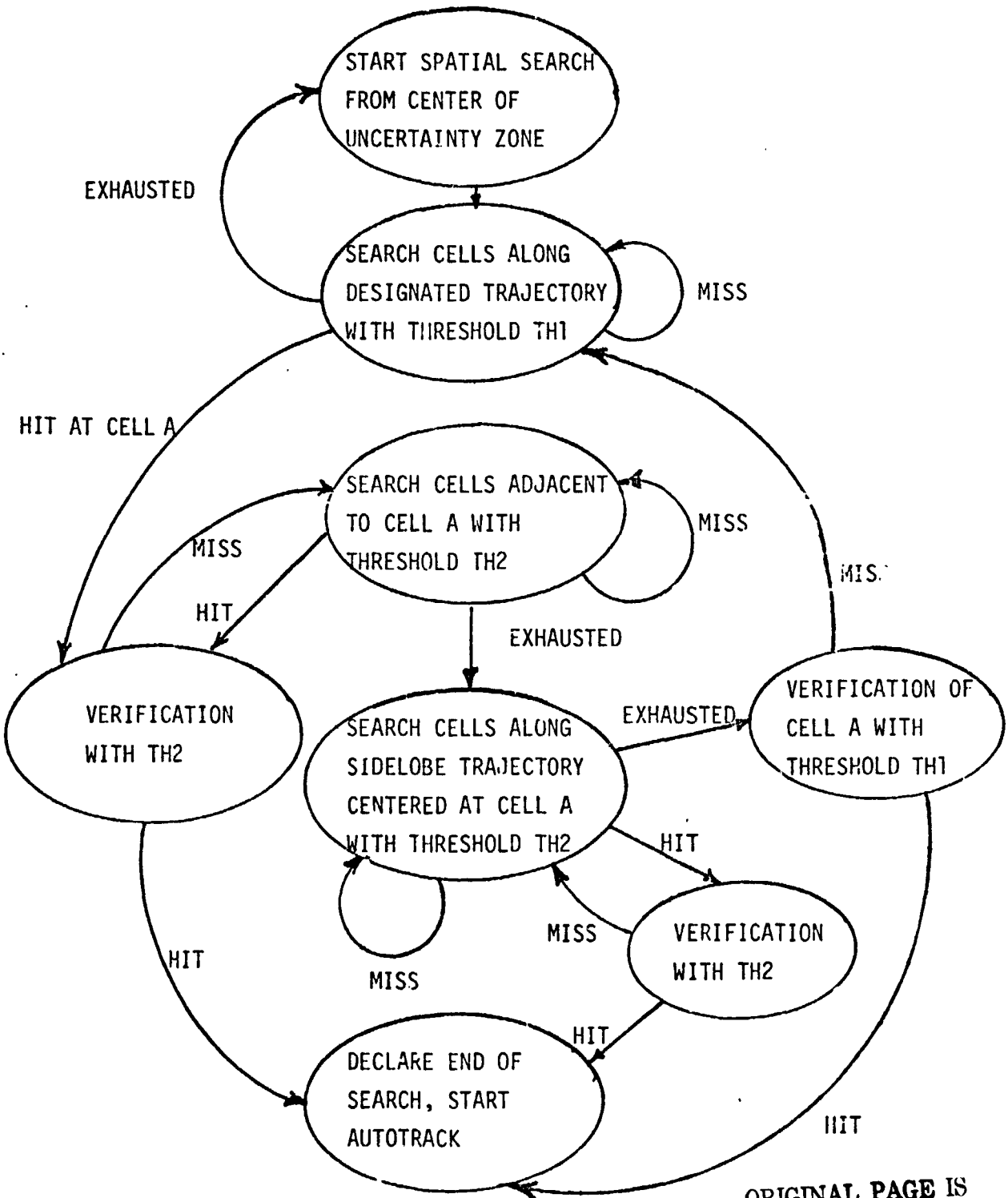

ORIGINAL PAGE IS
OF POOR QUALITY

On the other hand, if the threshold is exceeded, a hit is claimed and verification stage is entered. Once a second hit is obtained, the acquisition of the TDRS is declared and the procedure of the spatial search is stopped; otherwise, the search continues.

The second acquisition scheme is designed to exclude the sidelobe acquisition which occurs for large values of CNR. Two threshold levels are set up to distinguish the sidelobe acquisitions from the mainlobe ones. The following rules for two threshold levels are:

(1) For a specified probability of false-alarm, P_{fa} and an operating range of CNR, a threshold TH1 is computed at the lowest value of CNR.

(2) At the largest value of CNR, the second threshold TH2 against the detection due to the sidelobe of antennas is computed for the specified P_{fa}.

(3) The threshold level TH1 should be used initially in the stage of acquisition. Once a hit is indicated, threshold TH2 is used for a mini scan to verify any sidelobe acquisition.

The status of the second acquisition can be briefly classified into three stages--routine scan, mini-scan and verification. The procedure of the acquisition is similar to the normal scan, except that when a hit is indicated, the acquisition enters a mini-scan stage. The purpose of the mini-scan is to verify whether the hit H in the routine scan is caused by the main lobe of the antenna or by its sidelobe. The trajectory of the mini-scan is a circle centered at the position of the hit H with radius R = 2.5° (for θ_B = 0.8 degree of antenna),

which is the separation distance between the first sidelobe and the mainlobe, see Fig. 23. Regardless of hit or not after exhausting the mini-scan trajectory, the acquisition enters a verification stage, as indicated in Fig. 21.

There are two different cases for verification. First, the verification of a hit during mini-scan search requires no change in threshold level. If a second hit is observed during this verification stage, the search is terminated and the system enters autotrack mode for refine acquisition; otherwise, it returns to mini-scan. For the second case, in which no hit was observed in mini-scan, the antenna is moved back to the position of hit H in the routine scan for a verification. This case will lower the threshold level to TH1. If a hit still is observed, the acquisition procedure terminates and enters the autotrack mode; otherwise, the routine scan is resumed.

In addition to the strategy used in the second scheme, the third scheme will scan the cells adjacent to the hit H in routine scan to acquire the TDRS position within the beamwidth if the hit was caused by small offset from the TDRS position (it happens when the CNR is around 80 dB Hz). The signal energies received in the adjacent cells are compared and the cell with the strongest signal energy will be chosen as the right hit. If there is no hit in the adajcent cells, the system will proceed the mini-scan as proposed for the second scheme. The flow diagram of the third scheme is shown in Fig. 22.

(3) Performance of Acquisition Systems

The performance of the acquisition systems will be measured

ORIGINAL PAGE IS
OF POOR QUALITY

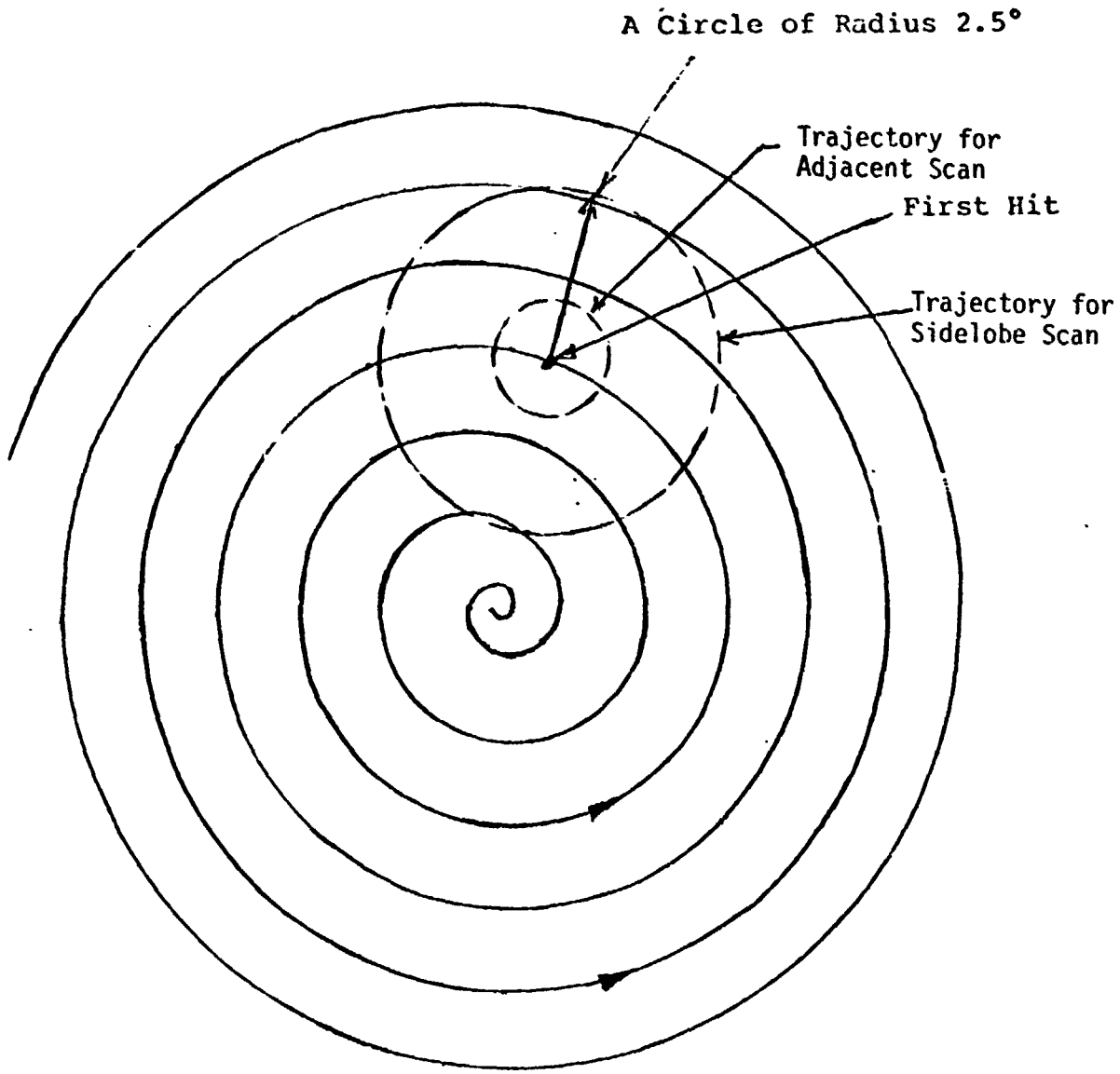

Figure 23. Trajectories for Normal Scan Plus Mini-Scans

by the average acquisition time in acquiring the TDRS position. The mathematical analysis of the acquisition performance is rather complicated because of the following reasons:

(1) Nonuniform probability distribution of the TDRS position.

(2) Nonuniform mechanical dwell time for each cell.

(3) Complicated acquisition stretegies, such as mini-scan and fine scan.

However, a computer simulation program was developed for the study of the performance of acquisitions for various system conditions such as the probability distribution of the TDRS position, trajectories of Shuttle antennas, motion along the trajectory, CNR, probability of false alarm, probability of detection and different acquisition schemes. Figs. 24-26 give the performance of typical acquisition systems obtained using the simulation program. The simulation program and its capabilities are documented in Volume II of this report.

The scan time required to acquire the TDRS position was obtained through Monte Carlo approach. There are 500 simulated TDRS positions for each run. The analytic results given in Figs. 20 and 21 have been closely verified through the simulation program for CNR = 60 dB-Hz and normal scan acquisition algorithm. In addition, the third acquisition algorithm with combination of constant angular velocity and the constant speed along a spiral trajectory was also tested. Their results are plotted in Fig. 26 (also in Table II) for CNR = 60 dB-Hz and CNR = 80 dB-Hz. In these cases, we assume that the transition from a normal scan

ORIGINAL PAGE IS
OF POOR QUALITY

Figure 24. Average Spatial Acquisition Time for Constant Angular Velocity.

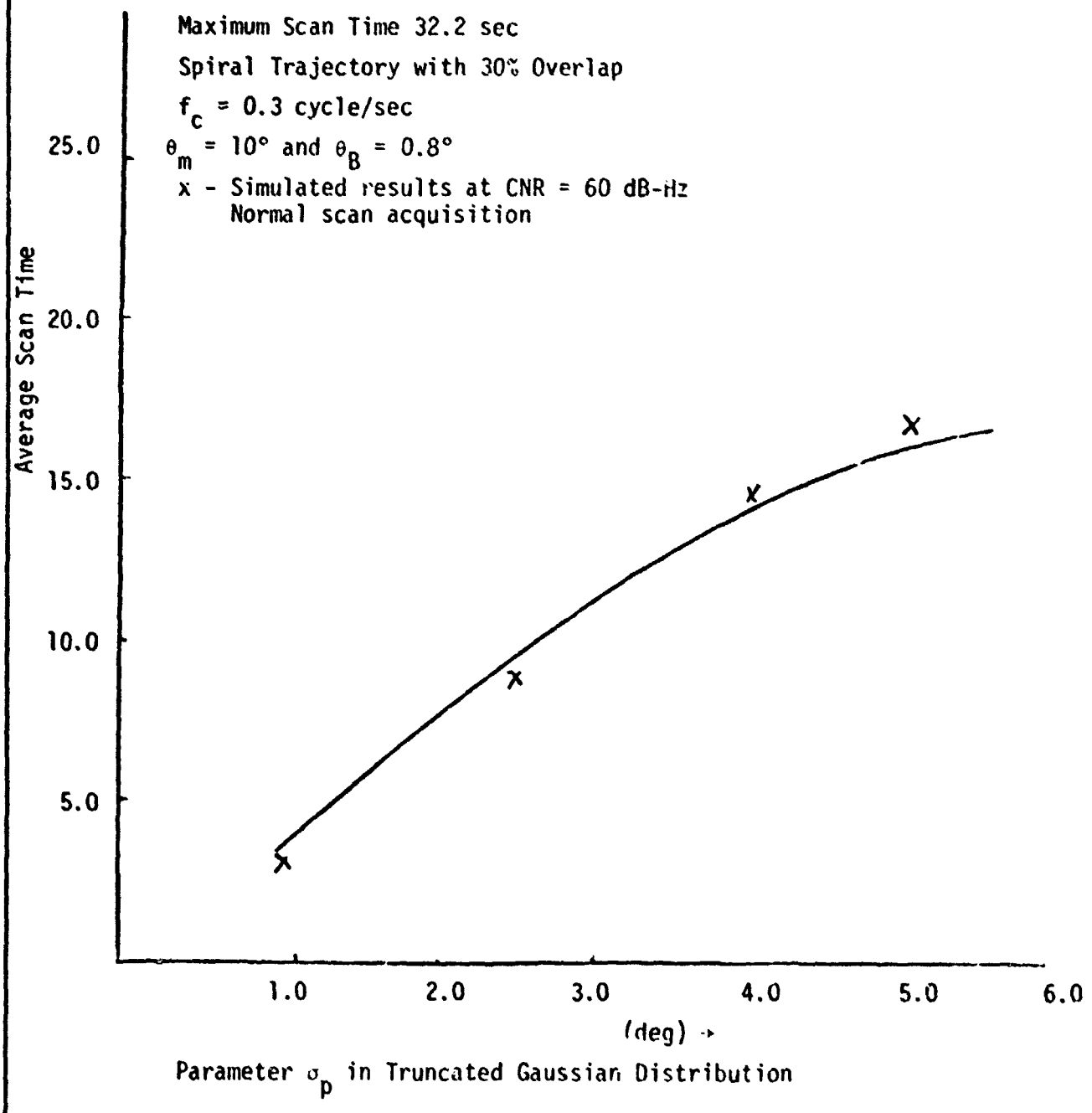

Figure 25. Average Spatial Acquisition Time for a Mixed Motion.

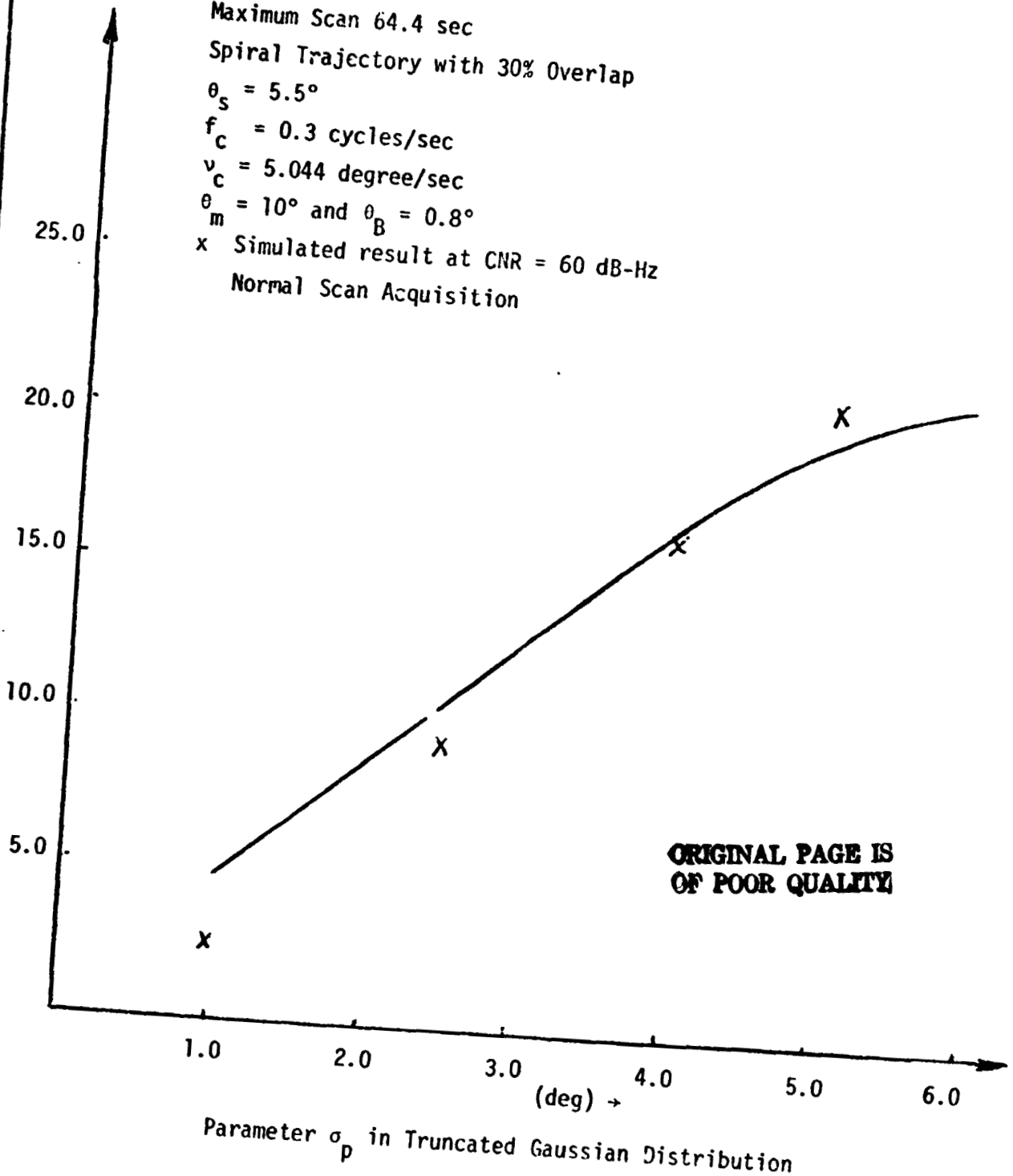

ORIGINAL PAGE IS
OF POOR QUALITY

LinCom

Figure 26. AVERAGE SPATIAL ACQUISITION TIME FOR THIRD ACQUISITION STRATEGY AND A MIXED MOTION ALONG SPIRAL TRAJECTORY OF 30% OVERLAP.

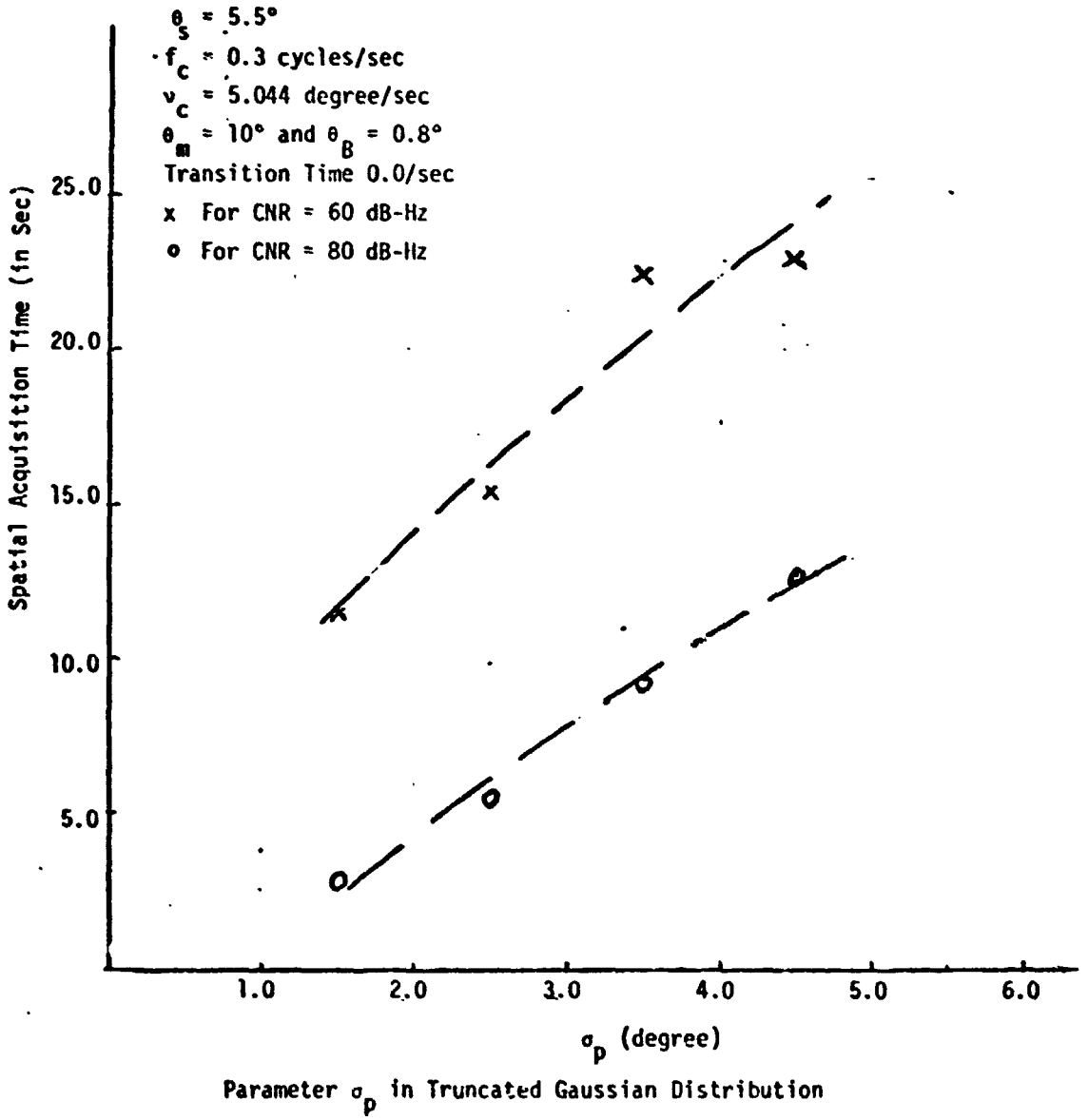

LinCom

to adjacent scan, or to sidelobe scan and vice versa, takes 0.0/sec and that motions along both the adjacent scan and the sidelobe scan are the constant angular velocity with respect to their scan center. It shows that at high CNR, the spatial acquisition is much shorter than that at a lower CNR, since the sidelobe scan and adjacent scan help shorten the scan time. Therefore, the third acquisition algorithm should be recommended for the consideration of the Ku-band acquisition system if the operating range of the CNR is wide, such as that used for this study, and if the side-lobe acquisition imposes a potential problem to the system performance.

ORIGINAL PAGE IS
OF POOR QUALITY

Table II. Acquisition Time for Third acquisition Algorithm with Mixed Motion Along a Spiral Trajectory of 30%.

σ_p	60 dB-Hz Average Scan Time	80 dB-Hz Average Scan Time
1.5	11.48	2.675
2.5	15.4	5.386
3.5	23.1	9.287
4.5	22.75	12.58

#·θ_m = 10°, θ_B = 1.6

·θ_s = 5.5°, f_c =0.3 cycle/sec, v_c = 5.044 degree/sec

VI. COMPUTER SIMULATION OF KU-BAND ANTENNA POINTING ACQUISITION SYSTEM

(1) Introduction

The Ku-band antenna pointing acquisition systems based on the noncoherent signal energy detection and scanning scheme discussed previously have been simulated by digital computers for the tradeoff study in the design of the Shuttle antenna acquisition. Several acquisition algorithms implemented are given to provide flexibility in accommodating the different operating ranges of autotrack systems. The acquisition strategies are primarily oriented toward the avoidance of the first side lobe acquisition in the spatial search. In addition, the simulation also provides various options on the scan trajectories, scan rates and a wide range of CNR. It essentially integrates the effect of interaction of spatial search acquisition schemes and the noncoherent signal energy detection. So the simulation program is able to support the design of hardware development.

The simulation program was written in Fortran IV for the Univac 1100 series computer. Originally, it was developed for time-shared operation, which is available at LINCOM Corporation. However, the program can also be used for batch processing with some modification. The program consists of 19 internal subroutine references and two external subroutines MERFIC (from IMSLS package) and BSSL (from MATHPACK) which are normally available for computer systems.

The computing time to run the simulation program depends on the number of tests on the TDRS position and the number of

samples taken for channel noises. These two variables are also provided as options for a user. The higher the values of these two variables, the higher the accuracy in predicting the acquisition performance and the longer the CPU time. The CPU time for a typical case is well within 10 sec if the number of noise samples is one and the number of simulated TDRS position is less than 500.

The simulation program provides various options for users to test system performance for a wide range of system parameters. The following options included are:

(1) The size of uncertainty cone of the TDRS position and its statistical distribution function over the cone.

(2) The antenna pattern of the Shuttle receiver (3 dB beamwidth).

(3) The types of antenna scan trajectories--square, hexagonal or spiral with different overlap.

(4) The scan rates--constant angular velocity, constant speed along a trajectory or combination of both previous cases (also a switching angle θ_s).

(5) The probability of false-alarm and the operating range of carrier-to-noise ratio (CNR).

(6) The receiver parameters--dwell time of the signal energy detector, IF filter bandwidth, insertion loss and other circuit losses.

(7) The number of TDRS positions used in the Monte Carlo simulation.

(8) The number of samples taken for channel noises.

(9) The types of acquisition algorithms.

ORIGINAL PAGE IS
OF POOR QUALITY

(10) The choices of a detailed printout or final results in the simulation.

The simulation program was structured as functional modules so that each subroutine can be easily replaced to adopt to any required function. For instance, the antenna pattern used in the simulation can be simply replaced by other types of antenna pattern. To do so, one should remove the subroutine ANTNNA and substitute an equivalent subroutine ANTNNA.

The simulation results are presented in two versions--one for a time-shared mode and the other for a batch process mode. For the time-shared mode, the computer asks for input data through interaction with users. A typical output generated by the simulation program consists of the following important parameters:

(1) The threshold TH1 and TH2 used for the signal energy detector in a normal scan and in mini scans (such as adjacent and sidelobe scans), respectively.

(2) Total number of cells to cover the whole uncertainty region.

(3) Maximum scanning time (= time spent to reach the last cell through normal path only).

(4) Average scanning time and corresponding standard deviation.

(5) "Probabilities" of detection, miss and false alarm.

A sample printout is given in Fig. 27.

(2) Functional Diagram of Simulation Program

To clarify the main functions performed in the simulation, a flow diagram of the simulation program is depicted in Fig. 28.

```
0
10.,1.6,3
30.
1
108.
1.e-3,60.,80.
60.,60.,1.
5.,6.,1.5,0.
500
1
1.,1.,1.
0
0.,0.,0.
0
2

RADIUS OF UNCERTAINTY REGION:                    10.0000 DEGREES
BEAMWIDTH:                                        1.6000 DEGREES
SPIRAL TRAJECTORY:              OVERLAP =        30.0000 %
CONSTANT ROTATIONAL SPEED:                      108.0000 DEGREES/S
PROBABILITY OF FALSE ALARM:                       .1000-02
CNR EXPECTED RANGE:                             60.0000 DB  -  80.0000 DB
INTEGRATION TIME:                                 5.0000 MS
IF FILTER BANDWIDTH:                              6.0000 MHZ
INSERTION LOSS:                                   1.5000 DB
OTHER LOSSES:                                      .0000 DB


THE PROBABILITY OF FALSE ALARM WAS RAISED TO 0.1 TO AVOID       SIDELOB
...E DETECTION
WHEN CNR = 80.00 DB/HZ



THRESHOLDS:   TH1 =  1.0568141     TH2 =  1.2276665

NUMBER OF CELLS:  302

MAXIMUM SCANNING TIME =  .3217689+02 SECONDS



NUMBER OF SATELLITE POSITIONS GENERATED:          500
STANDARD DEVIATION:                                .1000000+01

CARRIER-TO-NOISE RATIO:                            .6000000+02 DB
ACQUISITION AVERAGE TIME:                          .3023562+01 S
STANDARD DEVIATION:                                .2362385+01 S
PROBABILITY OF DETECTION:                          .1000000+01
PROBABILITY OF DETECTION (SL. VAR.):               .0000000
PROBABILITY OF MISS:                               .0000000
PROBABILITY OF FALSE ALARM (IN THE SIMULATION):    .0000000
```

ORIGINAL PAGE IS
OF POOR QUALITY

Figure 27a. A Sample of Input and Output Data.

Figure 27b. A SAMPLE OF INPUT DATA FOR BATCH PROCESSES

```
@bk1 ac\cd
BREAKPOINTED
>@tpf,u kuacq
@>@*Del*
>@xqt main
>0
>5.,1.6,2
>3
>108.,5.044,3
>1e-4,60.,80.
>60.,80.,20.
>5.,6.,1.5,0.
>5
>1
>2.5,2.5,1.
>1
>5
>1.e-3,1.e-3,5.e-3
>2
>2
>@bk2,u els
13 PAGES SYMMED BY HUANG.
>@fin
  RUNID: HUANG     ACCT: 0544AA
```

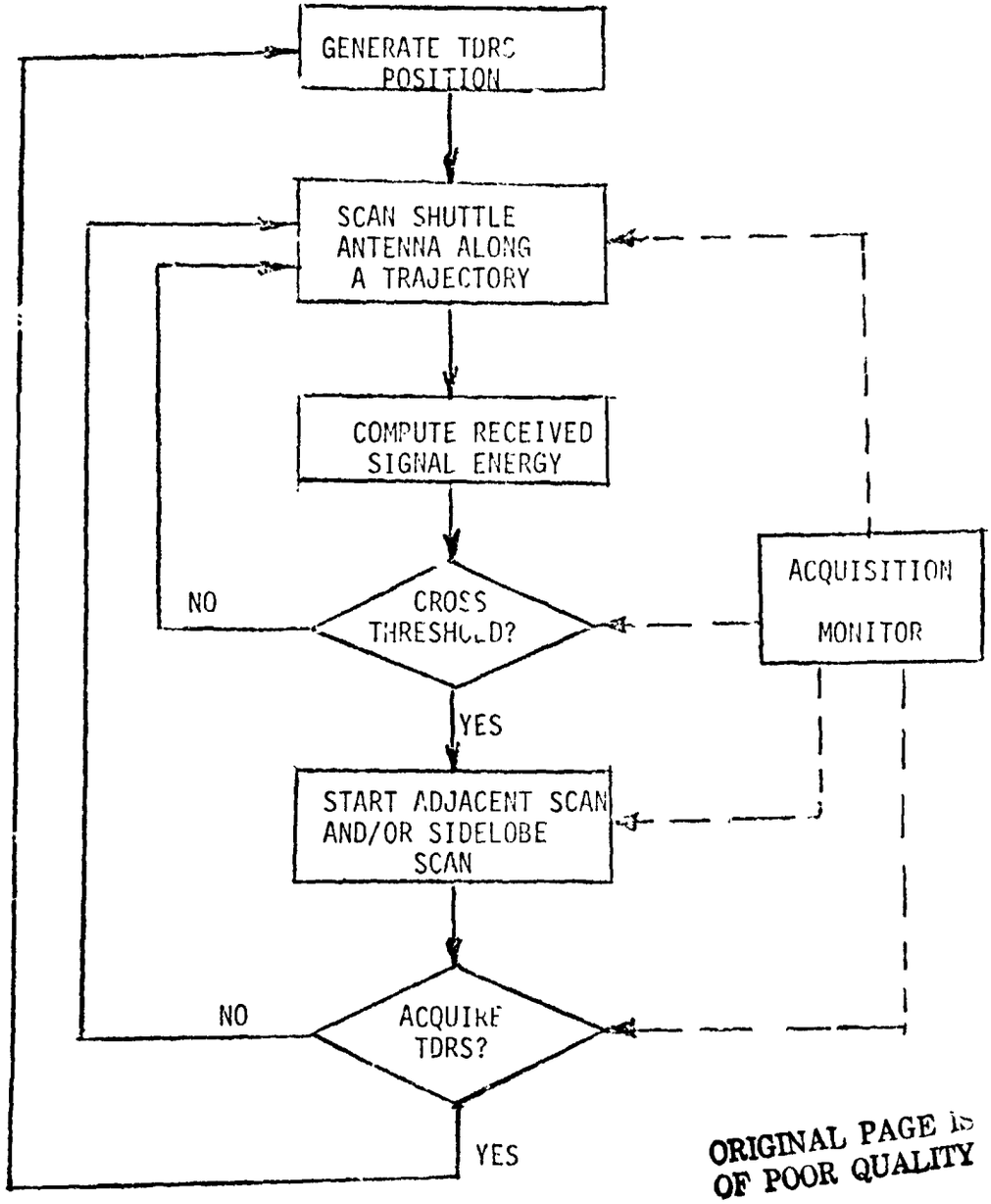

ORIGINAL PAGE IS OF POOR QUALITY

Figure 28. Functional Flow Diagram of the Simulation Program.

The TDRS position is simulated by a random generator with a specified distribution function. To measure the spatial acquisition time of the TDRS position, a set of simulated TDRS positions is tested for a specified trajectory and scan rates (speed for constant angular velocity and/or constant velocity along a trajectory). The simulated data reported here are all obtained by 500 simulated TDRS positions.

In the simulation program, the acquisition monitor is not a separate unit, but imbedded in the subroutine ACQ. This is implemented just for the convenience in programming. The detailed structure of the program is referred to Volume V.

(3) Capabilities of Software Package

The program developed for the Ku-band antenna pointing system provides various options in the size of uncertainty cone for the TDRS positions, the type of scanning and trajectories, and spatial acquisition algorithms. Here are the capabilities of the software package:

(1) Conical angle of the TDRS position can be 4°, 8° or 10°.

(2) The variance σ_p^2 of a priori probability distribution function of the TDRS position can vary from 0.1° to 10°.

(3) Antenna pattern can have beamwidth $\geq$ 10°.

(4) Three scan trajectories and wide range of scan rates (but limited by electrical dwell time) are available.

(5) The noncoherent signal detector can be operated over a wide range of CNR and $B_{IF}T$ product greater than 1000.

(6) Spatial acquisition algorithms with/without avoidance of sidelobe acquisition are selectable.

ORIGINAL PAGE IS
OF POOR QUALITY

(7) Probability of false alarm can be from 0.5 down to 10^{-7}.

(8) The number of TDRS positions in Monte Carlo simulation can be selected by users. But it is limited by the CPU time in executing the simulation program.

In addition, the software package also provides a useful feature for system designers to interact with a computer if the time-shared facility is available. Upon user's choices, a detailed spatial acquisition procedure can be printed out for a closed examination on the behavior of acquisition systems. Finally one should also note that the application of the software package should not be limited to the Ku-band system parameters even though it is oriented toward the study of Ku antenna pointing systems.

(4) Computer Program Utilization

The simulation program was designed for two modes of usage--batch process and time-shared modes. Since the computer program was originally developed through time-shared mode, it provides the mechanism of interactions between computers and users. However, this set of interactions should be suppressed for the batch processing. In order to run the program in batch, one should provide the same set of input data as one type in input data in the time-shared mode, except for the first input data. To illustrate the details of the input data required, several examples are given in Figs. 27 and 29 to show the options available in the simulation and the corresponding sets of input data for the batch process are also listed.

```
 IF YOU ARE ON-LINE, PLEASE TYPE 1
>1
 *** ON-LINE ***


 INPUT DATA   (FREE FORMAT)

 (REAL)  RADIUS OF UNCERTAINTY REGION        (DEGREES)
 (REAL)  BEAMWIDTH                           (DEGREES)
 (INTG)  TYPE OF TRAJECTORY:                 1(SQUARE)  2(HEXAGONAL)  3(SPIRAL)
>10.,1.6,1

 (INTG)  TYPE OF MOTION:
         1 - CONSTANT ANGULAR VELOCITY
         2 - CONSTANT VELOCITY ALONG TRAJECTORY
         3 - COMBINATION OF "1" AND "2"
>2

 (REAL)  ANGULAR VELOCITY (DEGREES/S)
 (REAL)  VELOCITY ALONG TRAJECTORY (DEGREES/S)
>108.,5.044

 (REAL)  PROBABILITY OF FALSE ALARM
 (REAL)  EXPECTED MINIMUM CARRIER-TO-NOISE RATIO (DB)
 (REAL)  EXPECTED MAXIMUM CARRIER-TO-NOISE RATIO (DB)
>1.e-4,60.,80.

         CNR VALUES TO BE USED IN THE SIMULATION
 (REAL)  (MINIMUM, MAXIMUM, INCREMENT.GE.0.)
>60.,80.,5.

         RECEIVER PARAMETERS:
 (REAL)  INTEGRATION TIME  (MS)
 (REAL)  IF FILTER BANDWIDTH  (MHZ)
 (REAL)  INSERTION LOSS  (DB)
 (REAL)  OTHER LOSSES  (DB)
>5.,6.,1.5,0.

 (INTG)  NUMBER OF SATELLITE POSITIONS TO BE GENERATED DURING THE SIMULATION
>500

 (INTG)  0 - SATELLITE POSITIONS ARE ENTERED AS INPUT DATA
         1 - SATELLITE POSITIONS ARE INTERNALLY GENERATED
>1

 (REAL)  STANDARD DEVIATION VALUES:  (MINIMUM, MAXIMUM, INCREMENT.GE.0.)  IN DEGREES
>2.5,2.5,1.

 (INTG)  INTERMEDIATE RESULTS:  NO(0)  YES(1)
>0

         TRANSITION MODES AND VERIFICATION TIMES:
 (REAL)  NORMAL TO SIDELOBE SCANNING
 (REAL)  NORMAL TO SURROUNDING CELLS SCANNING
 (REAL)  VERIFICATION TIME
>1.e-3,1.e-3,5.e-3

         SCANNING SCHEME:
 (INTG)  0 - NORMAL PATH ONLY
         1 - NORMAL PATH AND SIDELOBE CELLS
         2 - NORMAL PATH, NEARBY, AND THEN SIDELOBE CELLS
>0

 (INTG)  NUMBER OF NOISE SAMPLES   (EVEN  1<(.)<20 )
>
```

ORIGINAL PAGE IS
OF POOR QUALITY

Figure 29. A Sample Interaction Between a Computer and User.

```
 IF YOU ARE ON-LINE, PLEASE TYPE 1
>1
 *** ON-LINE ***



 INPUT DATA   (FREE FORMAT)

 (REAL)  RADIUS OF UNCERTAINTY REGION        (DEGREES)
 (REAL)  BEAMWIDTH                           (DEGREES)
 (INTG)  TYPE OF TRAJECTORY:                1(SQUARE)  2(HEXAGONAL)  3(SPIRAL)
>10.,1.6,3

 (REAL)  OVERLAP                             ( % )
>30.

 (INTG)  TYPE OF MOTION:
         1 - CONSTANT ANGULAR VELOCITY
         2 - CONSTANT VELOCITY ALONG TRAJECTORY
         3 - COMBINATION OF "1" AND "2"
>3

 (REAL)  ANGULAR VELOCITY (DEGREES/S)
 (REAL)  VELOCITY ALONG TRAJECTORY (DEGREES/S)
 (REAL)  SWITCHING ANGLE (DEGREES)
>108.,5.044,5.5


 (REAL)  PROBABILITY OF FALSE ALARM
 (REAL)  EXPECTED MINIMUM CARRIER-TO-NOISE RATIO (DB)
 (REAL)  EXPECTED MAXIMUM CARRIER-TO-NOISE RATIO (DB)
>1.e-3,60.,80.

         CNR VALUES TO BE USED IN THE SIMULATION
 (REAL)  (MINIMUM, MAXIMUM, INCREMENT.GE.0.)
>75.,75.,1.

         RECEIVER PARAMETERS:
 (REAL)  INTEGRATION TIME  (MS)
 (REAL)  IF FILTER BANDWIDTH  (MHZ)
 (REAL)  INSERTION LOSS  (DB)
 (REAL)  OTHER LOSSES  (DB)
>5.,6.,0.5,1.

 (INTG)  NUMBER OF SATELLITE POSITIONS TO BE GENERATED DURING THE SIMULATION
>1000

 (INTG)  0 - SATELLITE POSITIONS ARE ENTERED AS INPUT DATA
         1 - SATELLITE POSITIONS ARE INTERNALLY GENERATED
>1

 (REAL)  STANDARD DEVIATION VALUES:  (MINIMUM, MAXIMUM, INCREMENT.GE.0.)  IN DEGREES
>1.0,5.5,1.5

 (INTG)  INTERMEDIATE RESULTS:  NO(0)  YES(1)
>1

 (INTG)  HOW MANY RESULTS DO YOU WANT TO SEE IN DETAILS?
>30

         TRANSITION MODES AND      ICATION TIMES:
 (REAL)  NORMAL TO SIDELOBE SC      G
 (REAL)  NORMAL TO SURROUNDING      SCANNING
 (REAL)  VERIFICATION TIME
>1.e-3,1.e-3,5.e-3

         SCANNING SCHEME:
 (INTG)  0 - NORMAL PATH ONLY
         1 - NORMAL PATH AND      LOBE CELLS
         2 - NORMAL PATH AND      ALL THE SIDELOBE CELLS
>2

 (INTG)  NUMBER OF NOISE SA       (EVEN  1<(.)<20 )
>
```

Figure 29. (Cont'd)

```
 IF YOU ARE ON-LINE, PLEASE TYPE 1
>1
 *** ON-LINE ***



 INPUT DATA   (FREE FORMAT)

 (REAL)  RADIUS OF UNCERTAINTY REGION        (DEGREES)
 (REAL)  BEAMWIDTH                           (DEGREES)
 (INTG)  TYPE OF TRAJECTORY:                 1(SQUARE)  2(HEXAGONAL)  3(SPIRAL)
>10.,1.6,2

 (INTG)  TYPE OF MOTION:
         1 - CONSTANT ANGULAR VELOCITY
         2 - CONSTANT VELOCITY ALONG TRAJECTORY
         3 - COMBINATION OF "1" AND "2"
>1

 (REAL)  ANGULAR VELOCITY (DEGREES/S)
>108.

 (REAL)  PROBABILITY OF FALSE ALARM
 (REAL)  EXPECTED MINIMUM CARRIER-TO-NOISE RATIO (DB)
 (REAL)  EXPECTED MAXIMUM CARRIER-TO-NOISE RATIO (DB)
>1.e-4,60.,80.

         CNR VALUES TO BE USED IN THE SIMULATION
 (REAL)  (MINIMUM, MAXIMUM, INCREMENT.GE.0.)
>60.,80.,5.

         RECEIVER PARAMETERS:
 (REAL)  INTEGRATION TIME  (MS)
 (REAL)  IF FILTER BANDWIDTH  (MHZ)
 (REAL)  INSERTION LOSS  (DB)
 (REAL)  OTHER LOSSES  (DB)
>5.,6.,1.5,0.

 (INTG)  NUMBER OF SATELLITE POSITIONS TO BE GENERATED DURING THE SIMULATION
>10

 (INTG)  0 - SATELLITE POSITIONS ARE ENTERED AS INPUT DATA
         1 - SATELLITE POSITIONS ARE INTERNALLY GENERATED
>0

 (INTG)  INTERMEDIATE RESULTS:  NO(0)  YES(1)
>0

         TRANSITION MODES AND VERIFICATION TIMES:
 (REAL)  NORMAL TO SIDELOBE SCANNING
 (REAL)  NORMAL TO SURROUNDING CELLS SCANNING
 (REAL)  VERIFICATION TIME
>1.e-3,1.e-3,5.e-3

         SCANNING SCHEME:
 (INTG)  0 - NORMAL PATH ONLY
         1 - NORMAL PATH AND SIDELOBE CELLS
         2 - NORMAL PATH, NEARBY, AND FAR SIDELOBE CELLS
>1

 (INTG)  NUMBER OF NOISE SAMPLES   (EVEN  1<(.)<20 )
>4
```

ORIGINAL PAGE IS
OF POOR QUALITY

Figure 29. (Cont'd)

(5) Functional Descriptions of Subroutines

The functions of each subroutine used in the computer program for UNIVAC 1100 series are briefly described one-by-one here. Their flow charts and detailed documentations are given in Volume II separately. The description of subroutines is given in alphabetical order to be consistant with the computer printouts from UNIVAC 1108 time-shared mode. The program is, in fact started from MAIN then SIMULA. The subroutine SIMULA, the core of the simulation, cells and monitors the operations of the Monte Carlo simulation.

Subroutine ACQ

This simulates the acquisition algorithms discussed previously. The variable NULL, used to select the type of the acquisition algorithms for the simulation, is defined as follows:

NULL	=	0	for normal scan
		1	for normal scan plus sidelobe scan
		2	for normal scan, adjacent scan and sidelobe scan

In the process of the spatial acquisition, the time spent in any scan, including the transition from one scan to another and verification time, is accumulated as one of the outputs of the subroutine. The other important output parameters of the subroutine are:

(1) The status of the spatial search--success or failure (IPMISS and IPDET).

(2) How to acquire--the detection was declared by a normal scan or plus sidelobe scans (IPDSL).

(3) The acquired location of the TDRS (KHIT (IHIT)).

Subroutine ANTNNA

The antenna pattern of the simulated Shuttle receivers is assumed to have a first sidelobe of -175 dB from the peak of the main lobe. The antenna gain is computed from the offset angle between the simulated TDRS position and the boresight axis of the Shuttle. Hence, the offset angle (TH) is an input variable in addition to the parameters characterizing the antenna (THB, PATTC). A control variable K is used for computing the antenna parameters as shown here

K =	-2	for computing the angle of first null
	-1	for computing the angle of the peak of of the second sidelobe
	0	for computing the angle of the peak of the first sidelobe
	+1	for -3 dB beamwidth
	2	for normal usage in computing the gain of the antenna at offset TH.

Subroutine CELL

For a specified trajectory (KSCAN), the subroutine computes the locations of search cells (XCTR,YCTR) along the trajectory and the scan time to reach each search cell from the designated center of the uncertainty zone of the TDRS position. The scan time is computed by calling the subroutine TCENTR. Hence, it requires the following input variables

KSCAN =	1	for square trajectory
	2	for hexagonal trajectory
	3	for spiral trajectory

ORIGINAL PAGE IS
OF POOR QUALITY

MOTION = 1 for constant rotational speed

2 for constant speed along trajectory

3 for constant rotational speed first then constant speed along trajectory

VANG = angular velocity for constant rotational speed (in radian/sec)

VLIN = constant speed along trajectory (in radian/sec)

To ensure the electrical dwell time to be smaller than K_D times of the minimal mechanical dwell time, a warning is printed out if the antenna scan is too fast. In the subroutine K_D is set to be 1.0 .

Subroutine GAUSS

This is a Gauss random generator whose mean and standard deviation are specified by AVR and SIGMA, respectively. The Gaussian samples are obtained in pair by the following simple relations

$$y_1 = \sigma(-2.\ln x_1)^{1/2} \cos 2\pi x_2 + \mu$$

$$y_2 = \sigma(-2.\ln x_1)^{1/2} \sin 2\pi x_2 + \mu$$

where x_1 and x_2 are a pair of independent random variables uniformly distributed between 0 and 1, and μ and σ^2 are its mean and variance, respectively. The algorithm has been tested for its mean, variance and skew coefficient. The results show that the algorithm gives high confidence in its statistical nature.

Subroutine HIT

The signal energy detector is simulated by this subroutine. The received signal energy (sum of signal power and noise power)

is compared with a preset threshold (TH). If the threshold is crossed, a hit is declared (HIT=.TRUE.); otherwise, no hit is given. The input variables are the position of the TDRS and the location of the boresight axis of the Shuttle antenna. The offset angle ETA is computed, then the antenna gain by calling subroutine ANTNNA, the signal power and noise power.

Subroutine HPOSTN

This subroutine computes the centers of hexagonal cells along the hexagonal trajectory. The computation is proceeded from K^{th} cell to $(K+1)^{th}$ cell.

Subroutine ITR

This subroutine implements the iterative algorithm needed in solving for eqs. (20) and (21). The control variable K is used to indicate the application of the algorithm to eq. (20) or eq. (21).

MAIN

The function of the MAIN defines the dimension of variables used in the simulation. The program has been set to deal with the maximal number of search cells to be 500. If the number of the search cells goes beyond 500, one should expand dimensions of all variables in the first dimension statement.

MAIN/MAP

This is a set-up for executing the simulation program. Two system subroutine packages--MATHPACK and IMSL--are called to satisfy the external references.

ORIGINAL PAGE IS
OF POOR QUALITY

Subroutine NOISE

The simulated channel noise power at the output of the integrator

is computed here. The number of samples for equivalent Gaussian noises is set by the variable KNOISE.

Subroutine QPOSTN

It computes the center of $(K+1)^{\underline{th}}$ search cell from the known center of the $K^{\underline{th}}$ search cell along the square trajectory.

Subroutine SIMULA

This is the core of the simulation program. It reads in the data, prints the outputs and also monitors the operation of the program. The detailed operation of the subroutine is referred to in Volume V.

Subroutine SLCELL

The search cells alons a sidelobe trajectory and adjacent cells to a hit cell are computed here. The adjacent cells are structured as those for hexagonal cells. Hence, the number of the adjacent cells to be scanned is fixed as six. However, the number of cells for the sidelobe trajectory varies depending upon the type of trajectory used for normal scan.

Subroutine SPOSTN

It computes the center of $(K+1)^{\underline{st}}$ cell along a spiral trajectory from the known center of the $K^{\underline{th}}$ cell.

Subroutine TCENTR

It computes the scan time required for the Shuttle antenna to sweep along a trajectory to reach a spatial point in the uncertainty zone of the TDRS position. It requires to input the type of motion, scan rate (constant rotation and/or constant speed along a trajectory) and the coordinates of the point.

Subroutine TDRS

The subroutine generates a simulated TDRS position according to a specified Gaussian distribution. If a Gaussian sample falls outside the uncertainty zone of the TDRS position, it is discarded and another sample is taken. Its input variables are SIGMA, THM2, and its output variables XTDRS and YTDRS.

Subroutine TH1TH2

The setup of threshold levels used for spatial acquisition is done in this subroutine. The threshold TH1 is first computed for the given probability of false-alarm under the channel noise condition. Then it checks the probability of detection P_{fas} due to the second sidelobe of the Shuttle antenna at the maximal value of CNR in the specified operating range. If P_{fas} is larger than the given probability of false alarm, the threshold is adjusted to yield at least 0.1 probability of false alarm due to second sidelobe at the strongest CNR. This implies that the probability of false-alarm at lowest CNR is much smaller than the specified one.

The threshold TH2 is computed based on the assurance of having the specified probability of false alarm due to the first sidelobe at strongest CNR.

Subroutine UNIFOR

This is a uniform random generator over (0,1). A pair of output samples are generated for each cell.

VII. SUMMARY AND RECOMMENDATIONS

The Ku-band antenna pointing system has been discussed and simulated by digital computers. Through the analytical and experimental results presented in this report, one may lead to the conclusion that the spiral trajectories with various scan rates (mixed motion) should provide the flexibility for the Ku-band antenna spatial scan over the TDRS uncertainty region and that the third acquisition algorithm proposed should not only avoid the side-lobe acquisition problem, but also yields a shorter acquisition time especially when the received signal at the Shuttle is strong.

With the various options available in the software package developed for this study, one should be able to perform, with ease, tradeoff study on the system parameters to yield an "optimal" system performance.

ORIGINAL PAGE IS
OF POOR QUALITY